Original Article

Exendin-4, a glucagon-like peptide-1 receptor agonist, attenuates prostate cancer growth

Running title: Ex-4 attenuates prostate cancer growth

Takashi Nomiyama[1#], Takako Kawanami[1#], Shinichiro Irie[2], Yuriko Hamaguchi[1], Yuichi Terawaki[1], Kunitaka Murase[1], Yoko Tsutsumi[1], Ryoko Nagaishi[1], Makito Tanabe[1], Hidetaka Morinaga[1], Tomoko Tanaka[1], Makio Mizoguchi[3], Kazuki Nabeshima[3], Masatoshi Tanaka[2] and Toshihiko Yanase[1*]

[1]Department of Endocrinology and Diabetes Mellitus, School of Medicine, Fukuoka University, 7-45-1 Nanakuma, Jonan-ku, Fukuoka 814-0180, Japan
[2]Department of Urology, School of Medicine, Fukuoka University, 7-45-1 Nanakuma, Jonan-ku, Fukuoka 814-0180, Japan
[3]Department of Pathology, Faculty of Medicine, Fukuoka University, 7-45-1 Nanakuma, Jonan-ku, Fukuoka 814-0180, Japan

[*]**Correspondence**: Toshihiko Yanase MD., PhD. Department of Endocrinology and Diabetes Mellitus, School of Medicine, Fukuoka University, 7-45-1 Nanakuma, Jonan-ku, Fukuoka 814-0180, Japan
E-mail: tyanase@fukuoka-u.ac.jp

[#] These authors contributed equally to this work.

3,967 Words, 1 Table, 7 Figures

ABSTRACT

Recently, pleiotropic benefits of incretin therapy beyond glycemic control have been reported. Although cancer is one of the main causes of death in diabetic patients, few reports describe the anti-cancer effects of incretin. Here, we examined the effect of the incretin drug Exendin-4, a glucagon-like peptide-1 receptor (GLP-1R) agonist, on prostate cancer. In human prostate cancer tissue obtained from patients after radical prostatectomy, GLP-1R expression co-localized with P504S, a marker of prostate cancer. In in vitro experiments, Exendin-4 significantly decreased proliferation of the prostate cancer cell lines, LNCaP, PC3 and DU145, but not that of ALVA-41. This anti-proliferative effect depended on GLP-1R expression. In accordance with the abundant expression of GLP-1R in LNCaP cells, a GLP-1R antagonist or *GLP-1R* knockdown with siRNA abolished the inhibitory effect of Exendin-4 on cell proliferation. Although Exendin-4 had no effect on either androgen receptor activation or apoptosis, it decreased extracellular signal-regulated kinase (ERK)-mitogen-activated protein kinase (MAPK) phosphorylation in LNCaP cells. Importantly, Exendin-4 attenuated in vivo prostate cancer growth induced by transplantation of LNCaP cells into athymic mice and significantly reduced tumor expression of P504S, Ki67 and

phosphorylated ERK-MAPK. These data suggest that Exendin-4 attenuates prostate cancer growth through inhibition of ERK-MAPK activation.

Incretin therapy, which includes the delivery of dipeptidyl peptidase-4 inhibitors (DPP-4I) and glucagon-like peptide-1 receptor (GLP-1R) agonists, has become a popular treatment for type 2 diabetes. Recently, much attention has focused on incretin, because of its reported tissue-protective effects beyond lowering glucose levels (1). Diabetic patients have a higher risk of cardiovascular events compared with non-diabetic patients (2), and frequently experience restenosis after coronary angioplasty, even if intervention is performed with currently established drug-eluting stents (3). Accordingly, the potential of incretin-related anti-diabetic agents to improve not only glycemic control but also cardiovascular systems has been investigated. Indeed, the vascular-protective effects of Exendin-4 (Ex-4), a GLP-1R agonist, have been demonstrated by the attenuation of atheroma formation in apoE$^{-/-}$ mice via inhibition of NFκB activation in macrophages (4) and by the reduction in intimal thickening after vascular injury via 5' AMP-activated protein kinase (AMPK) activation in vascular smooth muscle cells (5). Thus, incretin therapy could improve the quality of life and mortality rate of patients with diabetes through its vascular-protective effects.

Cancer is another major cause of death in diabetic patients (6), especially, in Japan, where it is the leading cause of death in patients with type 2 diabetes (7). Subsequently, the Japan Diabetes Society and Japan Cancer Association have issued a

warning about increased risk of cancer in diabetic patients (8). Furthermore, the Hisayama study has suggested that not only diabetes but also impaired glucose tolerance increases the incidence of cancer-related deaths in the Japanese population (9). Specifically, diabetes has been suggested to be associated with higher risk of many malignancies, such as pancreatic (10), renal cell (11), colon (12) and breast (13) cancers.

Although numerous types of cancer have been recognized to be associated with diabetes and metabolic syndrome (14), the association between diabetes and metabolic syndrome with prostate cancer remains controversial (15-19). Indeed, diabetes has been associated with both advanced prostate cancer and prostate cancer mortality, but not with the total phenomena caused by prostate cancer. Moreover, a follow-up study of 2546 patients with prostate cancer, enrolled in the Physicians' Health Study (20), revealed that both high body-mass index and plasma C-peptide concentrations increased the risk of mortality (21). Furthermore, we have previously reported that insulin and insulin-like growth factor-1 (IGF-1) accelerate prostate cancer cell proliferation through androgen receptor (AR) activation by disrupting its direct interaction with Foxo1 (22). These data favor the hypothesis that insulin-resistance and hyperinsulinemia in pre- or early diabetic states and metabolic syndrome are associated with poor prognosis for

prostate cancer patients. Intensive treatment of diabetes is, therefore, a rationale for preventing cancer (23). In the present study, we examined the anti-cancer effect of anti-diabetic incretin treatment using Ex-4 in a prostate cancer model. We found that Ex-4 attenuated prostate cancer growth through inhibition of ERK-MAPK activation.

RESEARCH DESIGN AND METHODS

Human tissues

Human prostate cancer tissues were obtained from two non-diabetic prostate cancer patients (67 and 70 years old) after radical prostatectomy at the Fukuoka University Hospital. The tissues were paraffin-embedded, formalin-fixed and cut into 3-μm sections for immunofluorescent staining. All patients provided written informed consent for participation in this study. The study protocol was approved by the Ethics Committees of Fukuoka University Hospital.

Animals

Athymic CAnN.Cg-*Foxn1nu*/CrlCrlj mice were purchased from Charles River Laboratories (Yokohama, Japan) and housed in specific pathogen-free barrier facilities at Fukuoka University. Mice were treated with either saline (n = 7) or with Exendin-4

(Sigma-Aldrich, St Louis, MO, USA) at a high dose (24 nmol/kg body weight/day, n = 7) or a low dose (300 pmol/kg body weight/day, n = 8) delivered through a mini-osmotic pump (ALZEST, model 1004; DURECT, Cupertino, CA, USA) as described previously (4). At the age of 6 weeks, 1×10^6 LNCaP cells (passages 4–8) were mixed with 250 µl Matrigel (Becton Dickinson Labware, Bedford, MA, USA) and after local anesthesia they were transplanted subcutaneously into the flank region of each mouse while the osmotic pump was inserted under the dorsal skin. At the age of 12 weeks, blood samples were collected, and mice were euthanized. Tumors were extracted and their volume was calculated according to the modified ellipsoid formula: length × width^2 × 0.52, as previously reported (24). Paraffin-embedded formalin-fixed tumors were cut into 5-µm sections and prepared for immunofluorescent staining. All animal procedures were reviewed and approved by the Institutional Animal Care Sub-committee of Fukuoka University Hospital.

Cell culture and cell proliferation assays

The LNCaP human androgen-sensitive prostate cancer cell line, and PC3 and DU145 human androgen-independent prostate cancer cell lines, were purchased from the American Type Culture Collection (ATCC; Manassas, VA, USA). The ALVA-41

human androgen-sensitive prostate cancer cell line was kindly provided by Dr. Naito (Kyushu University). LNCaP, ALVA-41 and DU145 cells were maintained in RPMI 1640 media and PC3 cells were cultured in **Dulbecco's Modified Eagle Medium (DMEM): Nutrient Mixture F-12. All media were** supplemented with 10% FBS and 1% penicillin/streptomycin. Cell proliferation assays were performed as described previously (25) with minor modifications. Briefly, LNCaP (30000 cells/well), PC3 (60000 cells/well), ALVA-41 (30000 cells/well) and DU145 (30000 cells/well) cells were seeded in 12-well tissue culture plates and maintained in complete media with or without 0.1–10 nM Ex-4, 100 nM Exendin (9-39) (Bachem, Torrance, CA, USA), 10 μmol/l PKI_{14-22} (Sigma-Aldrich) or 10 μM PD98059 (Sigma-Aldrich). Cell proliferation was analyzed daily up to 4 days by cell counting using a hemocytometer. For all experiments, cells were used at passages 4 to 8. Experiments were performed in triplicate using five different cell preparations.

siRNA knockdown of *GLP-1R* expression and cell proliferation assay

To knockdown *GLP-1R*, we used Stealth RNAi Pre-Designed siRNA (Invitrogen, Carlsbad, CA, USA), which was designed for human *GLP-1R* (HSS104179-81), and Stealth RNAi Negative Control Duplexes (Invitrogen) were used

as a negative control. For transfection, LNCaP cells were plated at a density of 1×10^5 cells/well in 6-well plates and transfected with 1 nmol/l of *GLP-1R* siRNA or the negative control using MISSION® siRNA Transfection Reagent (Sigma-Aldrich). Twenty-four hours after transfection, cells were subjected to the cell proliferation assay. Briefly, cells were detached and re-plated in 24-well tissue culture plates in complete media with or without 10 nM Ex-4. Four days after the treatment, cells were collected and counted using a hemocytometer. The siRNA knockdown efficiency was confirmed by RT-PCR analysis of *GLP-1R* (Supplemental Fig. 2).

Reverse transcription and quantitative real-time RT-PCR

Total mRNA from prostate cancer cells was isolated using RNeasy Mini Kits (Qiagen, Venlo, the Netherlands) and reverse-transcribed into cDNA. PCR reactions were performed using Light Cycler 2.0 (Roche, Basel, Switzerland) and SYBR Premix Ex Taq™ II (Takara, Otsu, Japan). Each sample was analyzed in triplicate and normalized against TATA binding protein (*TBP*) mRNA expression. The primer sequences used were as follows: human *TBP*, 5′-TGCTGCGGTAATCATGAGGATA-3′ (forward), 5′-TGAAGTCCAAGAACTTAGCTGGAA-3′ (reverse); human *GLP-1R*,

5′-GGTTCATCTAGGGACACGTTAGGA-3′ (forward), 5′-GACAGCGTGTGGTCACAGATAAAG-3′ (reverse); and human *PSA*, 5′-CACCTGCTCGGGTGA-3′ (forward), 5′-CCACTTCCGGTAATGCACCA-3′ (reverse). To verify the mRNA expression of human *GLP-1R*, we also amplified the 890 bp coding sequence of human *GLP-1R* using RT-PCR, as previously reported (26). PCR products were separated by agarose gel electrophoresis and visualized with ethidium bromide staining.

Determination of cAMP concentration

Measurement of cAMP concentration was performed as described previously (5). Briefly, LNCap cells were plated in 96-well plates at a density of 1500 cells/well and cultured overnight. Next, they were serum deprived for 24 h and incubated with Ex-4 (10 nM) for 0, 15, 30 or 60 min. After incubation, the medium was aspirated and lysis buffer was added. Intracellular cAMP concentration ($[cAMP]_i$) was determined using the cAMP enzyme immunoassay (EIA) kit (GE Healthcare, Little Chalfont, UK) according to the manufacturer's instructions.

PSA measurements

Prostate serum antigen (PSA) protein concentrations in cell culture medium and mouse serum were measured using EIA at SRL Inc. (Tokyo, Japan).

Plasmids, transient transfections, and luciferase assays

To evaluate androgen receptor activation, the luciferase reporter assay was performed in LNCaP cells transiently transfected with the pGL3-MMTV or pPSA-LUC reporter constructs, as described previously (22). Briefly, LNCaP cells were transfected for 6–8 hours with 0.5 μg of reporter DNA using FuGENE HD transfection reagent (Roche). Next, cells were maintained in media supplemented with 10% dextran coated-charcoal-filtered FBS with or without Ex-4 (0.1–10 nM) for 12 h, followed by stimulation with 10^{-8} M 5α-dihydrotestosterone (DHT; Sigma-Aldrich) for 24 h. Luciferase activity was assayed using the dual luciferase reporter assay (Promega, Madison, WI, USA). Transfection efficiency was normalized to *Renilla* luciferase activity generated by co-transfection of cells with 10 ng/well pRL-SV40 (Promega).

BrdU assays

To evaluate LNCaP cell proliferation, the bromodeoxyuridine (BrdU) incorporation assay was performed using Cell Proliferation ELISA kits (1647229;

Roche Applied Science, Mannheim, Germany) as described previously (5). Briefly, LNCaP cells were plated at 3000 cells/well in 96-well culture plates in complete media. After attaining 60–70% confluence, LNCaP cells were treated with or without Ex-4 (0.1–10 nM) diluted in media with 10% FBS for 24 h. BrdU solution (10 μM) was added during the last 2 h of stimulation. Next, the cells were dried and fixed, and the cellular DNA was denatured with FixDenat solution (Roche Applied Science) for 30 min at room temperature (RT). A peroxidase-conjugated mouse anti-BrdU monoclonal antibody (Roche Applied Science) was added to the culture plates and incubated for 90 min at RT. Finally, tetramethylbenzidine substrate was added for 15 min at RT and absorbance of the samples was measured using a microplate reader at 450–620 nm. Mean data are expressed as a ratio of the control (non-treated) cell proliferation.

Apoptosis assays

For labeling nuclei of apoptotic cells, 1.2×10^5 LNCaP cells were plated on glass coverslips in Lab-Tek Chamber Slides (177380; Nunc, Thermo Scientific, Waltham, MA, USA) and fixed in 4% paraformaldehyde for 25 min. Terminal deoxynucleotidyl transferase-mediated dUTP nick end labeling (TUNEL) staining was performed using the DeadEnd fluorometric TUNEL system (Promega) according to the

manufacturer's protocol. During the final 24 h, LNCaP cells were incubated with 10 nM Ex-4. LNCaP cells treated with 1 unit/100 μl RQ1 RNase-Free DNase (M6101; Promega) for 24 h were used as a positive control. Triplicate independent experiments were conducted.

Immunohistochemistry

Paraffin sections were incubated with anti-GLP-1R antibody (NBP1-97308; Novus Biologicals, Littleton, CO, USA), anti-P504S antibody (IR060; Dako-Agilent Technologies, Santa Clara, CA, USA), anti-Ki67 antibody (ab66144; Abcam, Cambridge, UK) or anti-phospho-ERK-MAPK antibody (Thr-202/Tyr-204) (#4370; Cell Signaling, Danvers, MA, USA). Sections analyzed for GLP-1R and phospho-ERK-MAPK (Thr-202/Tyr-204) were subsequently incubated with Alexa Fluor 488 goat anti-rabbit IgG (A-11008; Life Technologies, Carlsbad, CA, USA), and sections analyzed for P504S and Ki67 were subsequently incubated with Alexa Fluor 546 goat anti-rabbit IgG (A-11010; Life Technologies). Sections were counterstained with DAPI and visualized by confocal microscopy.

Western blot analysis

Western blotting was performed as described previously (25). The following primary antibodies were used: phospho-ERK-MAPK (Thr-202/Tyr-204) (#9101; Cell Signaling) and ERK-MAPK (#9102; Cell Signaling). The expression of these proteins was examined in LNCaP cells that were incubated in media with 10% FBS and stimulated with or without 10 nM Ex-4 for 15 min, and pretreated for 30 min with or without 10 μmol/l of the protein kinase A (PKA) inhibitor, PKI_{14-22} (Sigma-Aldrich).

Statistical analysis

Unpaired *t*-tests and one-way analysis of variance (ANOVA) were performed for statistical analysis as appropriate. *P*-values less than 0.05 were considered to be statistically significant. Results are expressed as mean ± SEM.

RESULTS

GLP-1R is expressed in human prostate cancer tissue

To assess GLP-1R expression in prostate cancer we first performed immunohistochemical analysis of GLP-1R in human prostate cancer tissues. As shown in Figure 1, GLP-1R was abundantly expressed in human prostate cancer tissue, and co-localized with P504S/α-methylacyl-CoA racemase (AMACR), a marker of prostate

cancer (27). This observation suggests that GLP-1R is predominantly expressed in cancerous cells in the prostate. We observed a similar pattern of GLP-1R expression in at least three sections of prostate tissue obtained from two independent non-diabetic patients with prostate cancer. Because the sensitivity and specificity of the available anti-GLP-1R antibodies are currently under discussion (28), the specificity of the anti-GLP-1R antibody used in this study was confirmed using GLP-1R-overexpressing COS-7 cells (Supplemental Fig. 1). Drucker et al. (29) have demonstrated that the anti-GLP-1R antibody produced by Novus (1940002), but not that by Abcam (ab39072), can detect GLP-1R expression. We also tried to stain GLP-1R-overexpressing cells with the Abcam antibody, ab39072. However, we did not observe any staining (Supplemental Fig. 1).

Exendin-4 inhibits prostate cancer cell proliferation through GLP-1R

We next examined the in vitro effect of Ex-4 on the prostate cancer cell lines, LNCaP, PC3, ALVA-41 and DU145. LNCaP and ALVA-41 are androgen-dependent while PC3 and DU145 are androgen-independent. Treatment with Ex-4 (0.1–10 nM) significantly decreased the proliferation of LNCaP, PC3 and DU145 cells in a dose-dependent manner (Fig. 2A, B, D), although it had the strongest effect on LNCaP

cells. In contrast, Ex-4 did not affect the proliferation of ALVA-41 cells (Fig. 2C). To determine whether the anti-proliferative effect of Ex-4 on prostate cancer cells was mediated via GLP-1R, we examined its expression in these cells. Following a previous report (26), we first performed RT-PCR on the 890 bp coding sequence of *GLP-1R*, to confirm the exact expression of the gene. *GLP-1R* mRNA was abundantly expressed in LNCaP and DU145 cells, but was significantly lower in PC3 and ALVA-41 cells (Fig. 3A). Moreover, the sequence of the PCR product was compatible with that of the human *GLP-1R* cDNA as tested by direct sequencing. Quantitative real-time RT-PCR analysis further showed that *GLP-1R* expression was significantly higher in LNCaP cells, followed by DU145 cells, compared with that in the other tested cells (Fig. 3B). Consistently, immunohistochemistry analysis revealed that GLP-1R protein expression was also higher in LNCaP cells compared with that in the other tested cells. Indeed, counting the positively stained cells confirmed that GLP-1R protein expression was significantly greater in LNCaP cells, followed by DU145 cells, compared with that in the other cell lines (Fig. 3C). Accordingly, we speculated that the stronger suppression of cell proliferation by Ex-4 observed in LNCaP cells compared with that in the other prostate cancer cells was caused by its higher GLP-1R expression. Consequently, the subsequent experiments were conducted with LNCaP cells.

The anti-proliferative effect of Ex-4 was completely abolished by the GLP-1R antagonist, Exendin (9-39) in LNCaP cells (Fig. 4A). Similarly, when *GLP-1R* was partially knocked down with siRNA, Ex-4-induced inhibition of cell proliferation was significantly impaired ($P < 0.01$; Fig. 4B). These data suggest that Ex-4 inhibited prostate cancer cell proliferation through GLP-1R activation. To elucidate whether the detected GLP-1R in LNCaP cells can functionally activate downstream canonical signaling, we measured $[cAMP]_i$ following Ex-4 stimulation. Ex-4 significantly increased $[cAMP]_i$ in LNCaP cells (Fig. 4C), but not in the other cell lines, while the basal cAMP concentration was higher in PC3 cells (Supplemental Fig. 3), suggesting that GLP-1R is functionally intact and responsive to Ex-4 in LNCaP cells. Furthermore, the anti-proliferative effect of Ex-4 was canceled by the PKA inhibitor, PKI_{14-22} (Fig. 4D), and forskolin inhibited LNCaP cell proliferation (Supplemental Fig. 4A), suggesting that Ex-4 inhibits cell proliferation through the canonical GLP-1R signal.

Exendin-4 does not decrease androgen receptor activation

Prostate cancer cell proliferation depends mainly on androgen receptor (AR) activation. Thus, we investigated whether the anti-proliferative effects of Ex-4 are caused by decreased AR action. PSA is one of the most important targets of AR activation in prostate cancer cells. As shown in Figure 5A and B, DHT treatment

profoundly stimulated PSA mRNA and protein expression in LNCaP cells ($P < 0.01$) independently of Ex-4 concentration. However, while Ex-4 did not affect *PSA* mRNA expression, it significantly increased PSA protein production ($P < 0.01$). We next examined transcriptional activation of AR using a reporter assay. As described previously (22), pGL3-MMTV, which has multiple AR activation sites in its promoter region (30, 31), and the *PSA* promoter-Luc were transfected into LNCaP cells. As shown in Figure 5C and D, while the AR transactivation activity was dramatically induced by DHT, Ex-4 treatment had no effect. These data strongly suggest that Ex-4 inhibits prostate cancer cell proliferation in a manner independent of AR transactivation. We also performed these experiments with a lower dose of DHT, 10^{-9} M, and observed similar results to those in Figure 5A–D (data not shown).

Exendin-4 suppresses prostate cancer cell proliferation through inhibition of ERK-MAPK

We next examined the mechanism by which Ex-4 inhibits prostate cancer cell proliferation. First, we performed BrdU incorporation assays to assess DNA synthesis. Ex-4 treatment for 24 h significantly decreased DNA synthesis in LNCaP cells in a dose-dependent manner (Fig. 6A). However, Ex-4 did not induce apoptosis (Fig. 6B).

The ERK-MAPK pathway is one of the main signaling pathways that stimulate cell proliferation in prostate cancer cells (32). Therefore, we examined whether Ex-4 attenuates ERK-MAPK activation. Ex-4 significantly reduced ERK-MAPK activation as determined by western blot analysis of phosphorylated ERK1/2 in LNCap cells (Fig. 6C), but this effect was not observed in other prostate cancer cells (Supplemental Fig. 5). Next, we examined the effect of PKI on the inhibitory effect of Ex-4 on ERK-MAPK activation. As shown in Figure 6D, the inhibitory effect of Ex-4 on ERK-MAPK activation was completely abolished by PKI. Moreover, forskolin inhibited ERK-MAPK phosphorylation in LNCaP cells (Supplemental Fig. 5B). Interestingly, Ex-4 further inhibited LNCap cell proliferation when co-incubated with 10 μM PD98059 (Fig. 6E), a MAPK/ERK kinase (MEK) inhibitor, and a higher dose of PD98059 completely abolished LNCap cell proliferation regardless of the Ex-4-induced anti-proliferative effect (Supplemental Fig. 4B), suggesting that the Ex-4-induced inhibition of ERK-MAPK is independent of MEK inhibition.

These data indicate that Ex-4 suppresses prostate cancer cell proliferation mainly through inhibition of ERK-MAPK via the cAMP-PKA pathway, but does not induce apoptosis.

Exendin-4 attenuates prostate cancer growth in vivo

Finally, to examine the anti-prostate cancer effect of Ex-4 in vivo, we transplanted LNCaP cells into athymic mice. Six weeks after subcutaneous transplantation of LNCaP cells into the flank region of mice, massive tumor formation was observed. However, tumor size was dramatically decreased in mice treated with Ex-4 (Fig. 7A). Calculation of tumor size using the modified ellipsoid formula revealed that Ex-4 decreased tumor size to almost half that of the control (Fig. 7B). As shown in Table 1, body weight and blood glucose levels were not changed by Ex-4 treatment. Compared with the control, plasma PSA levels were decreased in mice treated with Ex-4, although this effect was not statistically significant (control vs. low dose, P = 0.11; control vs. high dose, P = 0.08). Immunohistochemical analysis of paraffin-embedded sections of subcutaneous prostate cancer tumors demonstrated that the expression of P504S, a marker of prostate cancer, dramatically decreased by Ex-4 treatment (Fig. 7C). Quantification of P504S expression based on the mean number of P504S-positive cells divided by the total number of nuclei confirmed that there was a significant dose-dependent decrease in P504S expression in tumors of Ex-4-treated mice compared with control mice (Fig. 7D). We next examined the expression of Ki67, a marker of cell proliferation and cell cycle progression. Ki67 expression, which was

clearly localized within the nucleus, was suppressed by Ex-4 treatment in a dose-dependent manner (Fig. 7E and F). Furthermore, consistent with our in vitro data, phosphorylated ERK-MAPK was decreased by Ex-4 treatment (Fig. 7G), which occurred in a dose-dependent manner (Fig. 7H). In addition, GLP-1R expression was not changed by Ex-4 treatment in vivo (Fig. 7I). These data suggest that Ex-4 attenuates prostate cancer growth in vivo by the same mechanism that was observed in vitro, i.e., through inhibition of ERK-MAPK signaling.

Discussion

In the present study, we clearly demonstrated that GLP-1R is expressed in human prostate cancer and that the GLP-1R agonist Ex-4 attenuates prostate cancer growth through inhibition of ERK-MAPK activation both in vivo and in vitro. Recently, incretin therapy, which includes GLP-1R agonists and DPP-4I, has become a popular anti-diabetic treatment throughout the world (33), including Japan (34). There are many benefits of incretin therapy, such as pancreatic β-cell preservation, lower risk of weight gain, and fewer hypoglycemic attacks (35). In addition, incretin is a therapeutic option for type 2 diabetes, even during end-stage renal disease (36). Furthermore, incretin therapy is expected to have tissue-protective effects beyond its glucose lowering

capacity (1). However, the current considerable interest in incretin therapy has raised the issue of its long-term safety including the risk of carcinogenesis.

In a previous report, a 13-week continuous exposure to liraglutide, a GLP-1R agonist, was associated with a marked increase in plasma calcitonin levels and thyroid C-cell hyperplasia in wild-type mice, but not in GLP-1R-deficient mice (37). Furthermore, GLP-1R expression has been detected in human neoplastic hyperplastic lesions of thyroid C cells (38). Thus, it can be speculated that these reports warn of a risk of carcinogenesis associated with incretin therapy. In contrast, two other studies have demonstrated an anti-cancer effect of a GLP-1R agonist (26,39), similar to that demonstrated in our study. Indeed, Koehler et al. have clearly demonstrated an anti-colon cancer effect of Ex-4 (26). Specifically, Ex-4 has been shown to increase intracellular cAMP levels and inhibit glycogen synthase kinase 3 and ERK-MAPK activation, leading to decreased colony formation and augmented apoptosis induced by irinotecan, a topoisomerase I inhibitor, in CT26 murine colon cancer cells (26). The cAMP-PKA pathway is a canonical signal transduction pathway downstream of GLP-1R, whose relationship with the ERK-MAPK pathway and cAMP is very complicated (40). Indeed, while induction of intracellular cAMP activates ERK-MAPK in some cell types, it inhibits it in others. In fact, GLP-1R signaling does not attenuate

ERK-MAPK signaling in pancreatic cancer (41). In the present study using prostate cancer cells, the inhibitory effect of Ex-4 on ERK-MAPK activation was mediated by the cAMP-PKA pathway. This was demonstrated by the significantly increased cAMP levels in the highly GLP-1R-positive LNCaP cells treated with Ex-4 (Fig. 4C), and by the PKI suppression of the Ex-4-mediated inhibition of ERK-MAPK (Fig. 6D).

In our previous study, we have observed that Ex-4 decreased vascular smooth muscle cell proliferation through AMPK activation (5), which is one of the mechanisms by which prostate cancer cell growth is inhibited (42). However, Ex-4 did not induce AMPK activation in prostate cancer cells (data not shown). Interestingly, an anti-breast cancer effect of Ex-4 has been recently reported (39). A similar mechanism by which Ex-4 attenuates cancer growth, namely inhibition of ERK-MAPK, was confirmed by our data and a previous report (26), suggesting the importance of ERK-MAPK as a target of Ex-4 for decreasing cancer growth.

We also examined the effect of Ex-4 on another growth signal in prostate cancer, Akt phosphorylation, however Ex-4 did not alter Akt activation in prostate cancer cells (Supplemental Fig. 6). Possibly there is a MEK-ERK-MAPK independent inhibitory mechanism by which Ex-4 inhibits prostate cancer cell proliferation, because PD98059 did not abolish the anti-proliferative effect of Ex-4 (Fig. 6E), and a higher

dose of PD98059 completely abolished prostate cancer cell proliferation (Supplemental Fig. 4B). However, our data suggest that Ex-4 inhibits prostate cancer cell proliferation mainly through ERK-MAPK inhibition. To fully elucidate the mechanism, further investigations are required.

We also observed that while Ex-4 inhibited prostate cancer cell proliferation it did not affect apoptosis as determined by the TUNEL assay (Fig. 6B). Indeed, further examination by western blot analysis confirmed that Ex-4 did not affect apoptosis signals, such as caspase 3 activation, and induction of Bcl-2 and Bad, (Supplemental Fig. 6).

In addition, we observed that Ex-4 increased PSA protein expression in LNCaP cells (Fig. 5B). The underlying molecular mechanism was not elucidated in this study; however, we have previously reported (22) that an interaction between GLP-1R signaling and Foxo1 may mimic AR activation, and another report has demonstrated that Ex-4 induced the translocation of Foxo1 from the nucleus to the cytoplasm (43). Further study is thus required to explain how Ex-4 increased PSA protein levels.

In conclusion, we detected GLP-1R expression in human prostate cancer tissues and cell lines, and demonstrated that Ex-4, a GLP-1R agonist, could attenuate prostate cancer growth through inhibition of ERK-MAPK activation.

Competing interests

The authors declare that they have no competing interests concerning this project.

Acknowledgments: TN performed experiments, wrote the manuscript and conceived the research hypothesis; TK and YH performed experiments; SI, MT, MM and KN provided the human prostate cancer tissues; YT, KM, YT, RN, MT and TT reviewed and edited the manuscript and assisted in patient recruitment; TY assisted in conception of the research hypothesis and reviewed and edited the manuscript. All authors read and approved the final manuscript. TY is the guarantor of this work and, as such, had full access to all the data in the study, and takes responsibility for the integrity of the data and the accuracy of the data analysis.

REFERENCES

1. Ussher JR, Drucker D. Cardiovascular biology of the incretin system. Endocr Rev 2012;33:187-215
2. Haffner SM, Lehto S, Ronnemaa T, Pyorala K, Laakso M. Mortality from coronary heart disease in subjects with type 2 diabetes and in nondiabetic subjects with and without prior myocardial infarction. N Eng J Med 1998;339:229-234
3. Scheen AJ, Warzee F. Diabetes is still a risk factor for restenosis after drug-eluting stent in coronary arteries. Diabetes Care 2004;27:1840-1841
4. Arakawa M, Mita T, Azuma K, et al. Inhibition of monocyte adhesion to endothelial cells and attenuation of atherosclerotic lesion by a glucagon-like peptide-1 receptor agonist, exendin-4. Diabetes 2010;59:1030-1037
5. Goto H, Nomiyama T, Mita T, et al. Exendin-4, a glucagon-like peptide-1 receptor agonist, reduces intimal thickening after vascular injury. Biochem Biophys Res Commun 2011; 405:79-84
6. Emerging Risk Factors Collaboration, Seshasai SR, Kaptoqe S, et al. Diabetes mellitus, fasting glucose, and risk of cause-specific death. N Engl J Med 2011;364:829-841
7. Hotta N, Nakamura J, Iwamoto Y, et al. Cause of death in Japanese diabetics based on the results of a survey of 18,385 diabetics during 1991-200 –report of committee on cause of death in diabetes mellitus- J Japan Diab Soc 2007;50:47-61 (in Japanese)
8. Kasuga M, Ueki K, Tajima N, et al. Report of the JDS/JCA joint committee on diabetes and cancer. Diabetol Int 2013;4:81-96
9. Hirakawa Y, Ninomiya T, Mukai N, et al. Association between glucose tolerance level and cancer death in a general Japanese population. Am J Epidemiol 2012;176:856-864
10. Morrison M. Pancreatic cancer and diabetes. Adv Exp Med Biol 2012;771:229-239
11. Joh HK, Willet WC, Cho E. Type 2 diabetes and the risk of renal cell cancer in woman. Diabetes Care 2011;34:1552-1556
12. Yuhara H, Steinmaus C, Cohen SE, Corley DA, Tei Y, Buffler PA. Is diabetes mellitus an independent risk factor for colon cancer and rectal cancer? Am J Gastroenterol 2011;106:1911-1921
13. Xue F, Michels KB. Diabetes, metabolic syndrome, and breast cancer: a review of the current evidence. Am J Clin Nutr 2007;86:s823-835

14. Esposito K, Chiodini P, Colao A, Lenzi A, Giugliano D. Metabolic syndrome and risk of cancer: a systemic review and meta-analysis. Diabetes Care 2012;35:2402-2411
15. Grossmann M, Wittert G. Androgens, diabetes and prostate cancer. Endocr Relat Cancer 2012;19:F47-62
16. Kasper JS, Liu Y, Giovannucci E. Diabetes mellitus and risk of prostate cancer in the health professionals follow-up study. Int J Cancer 2009;124:1398-1403
17. Bonovas S, Filloussi K, Tsantes A. Diabetes mellitus and risk of prostate cancer: a meta-analysis. Diabetologia 2004;47:1071-1078
18. Mitin T, Chen MH, Zhang Y, et al. Diabetes mellitus, race and the odds of high grade prostate cancer in men treated with radiation therapy. J Urol 2011;186:2233-2237
19. Moses KA, Utuama OA, Goodman M, Issa MM. The association of diabetes and positive prostate biopsy in a US veteran population. Prostate Cancer Prostatic Dis 2012;15:70-74
20. Final report on the aspirin component of the ongoing Physicians' Health Study. Steering Committee of the Physicians' Health Study Research Group. N Engl J Med 1989;321:129-135
21. Ma j, Li H, Giovannucci E, et al. Prediagnostic body-mass index, plasma C-peptide concentration, and prostate cancer-specific mortality in men with prostate cancer: a long-term survival analysis. Lancet Oncol 2008;9:1039-1047
22. Fan W, Yanase T, Morinaga H, et al. Insulin-like growth factor 1/insulin signaling activates androgen signaling through direct interactions of Foxo1 with androgen receptor. J Biol Chem 2007;282;7329-7338
23. Eyre H, Kahn R, Robertson RM; American Cancer Society, the American Diabetes Association, and the American Heart Association. Collaborative Writing Committee. Preventing cancer, cardiovascular disease, and diabetes: a common agenda for the American Cancer Society, the American Diabetes Association, and the American Heart Association. Diabetes Care 2004;27:1812-1824
24. Gupta S, Wang Y, Ramos-Garcia R, Shevrin D, Nelson JB, Wang Z. Inhibition of 5α-reductase enhances testosterone-induced expression of U19/Eaf2 tumor suppressor during the regrowth of LNCaP xenograft tumor in nude mice. Prostate 2010;70:1575-1585
25. Nomiyama T, Nakamachi T, Gizard F, et al. The NR4A orphan receptor NOR1 is induced by platelet-derived growth factor and mediates vascular smooth muscle cell proliferation. J Biol Chem 2006;281:33467-33476

26. Koehler JA, Kain T, Drucker DJ. Glucagon-like peptide-1 receptor activation inhibits growth and augments apoptosis in murine CT26 colon cancer cells. Endocrinology 2011;152:3362-3372
27. Jiang Z, Woda BA, Rock KL, et al. P504S: a new molecular marker for the detection of prostate carcinoma. Am J Surg Pathol 2001;25:1397-1404
28. Pyke C, Knudsen LB. The glucagon-like peptide-1 receptor-or not? Endocrinology 2013;154:4-8
29. Drucker DJ. Incretin action in the pancreas: potential promise, possible perils, and pathological pitfalls. Diabetes 2013;62:3316-3323
30. Ham J, Thomson A, Needham M, Webb P, Parker M. Characterization of response elements for androgens, glucocorticoids and progestins in mouse mammary tumour virus. Nucleic Acids Res 1988;16:5263-5276
31. Adachi M, Takayanagi R, Tomura A, Androgen-insensitivity syndrome as a possible coactivator disease. N Eng J Med 2000;343:856-862
32. Rodriguez-Berriguete G, Fraile B, Martinez-Onsurbe P, Olmedilla G, Paniagua R, Royuela M. MAP kinase and prostate cancer. J Signal Transduct 2012;2012: 169170–169178
33. Mikhail N. Safety of dipeptidyl peptidase 4 inhibitors for treatment of type 2 diabetes. Curr Drug Saf. 2011;6:304-309
34. Nomiyama T, Akehi Y, Takenoshita H, et al. Contributing factors related to efficacy of the dipeptidyl peptidase-4 inhibitor sitagliptin in Japanese patients with type 2 diabetes. Diabetes Res Clin Pract 2012;95:e27-28
35. Drucker DJ. Enhancing incretin action for the treatment of type 2 diabetes. Diabetes Care 2003;26:2929-2940
36. Terawaki Y, Nomiyama T, Akehi Y, et al. The efficacy of incretin therapy in patients with type 2 diabetes undergoing hemodialysis. Diabetology and Metab Synd 2013;5:10
37. Madsen LW, Knauf JA, Gotfredsen C, et al. GLP-1 receptor agonists and the thyroid : C-cell effects in mice are mediated via the GLP-1 receptor and not associated with RET activation. Endocrinology 2012;153:1538-1547
38. Gier B, Butler PC, Lai CK, et al. Glucagon-like peptide-1 receptor expression in the human thyroid gland. J Clin Endocrinol Metab 2012;97:121-131
39. Ligumsky H, Wolf I, Israeli S, et al. The peptide-hormone glucagon-like peptide-1 activates cAMP and inhibits growth of breast cancer cells. Breast Cancer Res Treat 2012;132:449-461

40. Stork PJ, Schmit JM. Crosstalk between cAMP and MAP kinase signaling in the regulation of cell proliferation. TRENDS in Cell Biol 2002;12:258-266
41. Koehler JA, Drucker DJ. Activation of glucagon-like peptide-1 receptor signaling does not modify the growth or apoptosis of human pancreatic cancer cells. Diabetes 2006;55:1369-1379
42. Zadra G, Priolo C, Patnaik A, Loda M. New strategies in prostate cancer: targeting lipogenic pathways and the energy sensor AMPK. Clin Cancer Res 2010;16:3322-3328
43. Kodama S, Toyonaga T, Kondo T, et al. Enhanced expression of PDX-1 and Ngn3 by exendin-4 during b cell regeneration in STZ-treated mice. Biochem Biophys Res Commun 2005;327:1170-1178

Figure legends

FIG. 1. Expression of the GLP-1 receptor in human prostate cancer tissue. Paraffin-embedded serial sections of human prostate cancer tissue obtained from non-diabetic prostate cancer patients were stained for the GLP-1 receptor and P504S, and counterstained with DAPI. Magnification, ×630.

FIG. 2. Exendin-4 inhibits prostate cancer cell proliferation via the GLP-1 receptor. (A) LNCaP cells, (B) PC3 cells, (C) ALVA-41 cells and (D) DU145 cells were maintained in the recommended media supplemented with 10% FBS with or without Ex-4 (0.1–10 nM). After 0, 24, 48, 72 and 96 h, the cells were harvested, and cell proliferation was analyzed by cell counting using a hemocytometer. Black circles with solid line = control (non-treated); black squares with dotted line = Ex-4 (0.1 nM); white circles with solid line = Ex-4 (1 nM); white squares with dotted line = Ex-4 (10 nM). One-way ANOVA was performed to calculate statistical significance ($^{*}P < 0.05$ vs. control; $^{**}P < 0.01$ vs. control).

FIG. 3. GLP-1R expression in prostate cancer cells

(A) RT-PCR was performed to examine mRNA levels of an 890 bp *GLP-1R* open reading frame. *TBP* was used as an input control. (B) Quantitative RT-PCR was

performed using a set of primers targeting exon 13 of *GLP-1R*. *TBP* expression was used for normalization. Unpaired *t*-tests were performed to calculate statistical significance ($^{**}P < 0.01$ vs. LNCaP; $^{\#\#}P < 0.01$ vs. DU145). (C) Immunohistochemistry was performed to examine GLP-1R expression in prostate cancer cell lines. All samples were counterstained with DAPI (magnification, ×400). (D) GLP-1R-positive cells were counted and normalized against DAPI in four individual fields-of-view. Unpaired *t*-tests were performed to calculate statistical significance ($^{**}P < 0.01$ vs. LNCaP; $^{\#\#}P < 0.01$ vs. DU145).

FIG. 4. Exendin-4 attenuates prostate cancer cell proliferation through GLP-1R. (A) LNCaP cells were maintained in media supplemented with 10% FBS with or without 10 nM Ex-4 or 100 nM Exendin (9-39). After 0, 24, 48, 72 and 96 h, the cells were harvested, and cell proliferation was analyzed by cell counting using a hemocytometer. Black circles with solid line = control (non-treated); black squares with dotted line = Ex-4 (10 nM); white circles with solid line = Exendin (9-39) (100 nM); white squares with dotted line = Ex-4 (10 nM) + Exendin (9-39) (100 nM). One-way ANOVA was performed to calculate statistical significance ($^{**}P < 0.01$ vs. control). (B) LNCaP cells were transfected with either negative control duplexes or *GLP-1R* siRNA

and maintained in media supplemented with 10% FBS with or without 10 nM Ex-4. After 0 or 96 h, the cells were harvested, and cell proliferation was analyzed by cell counting using a hemocytometer. One-way ANOVA was performed to calculate statistical significance ($^{**}P < 0.01$ vs. control without Ex-4). (C) Intracellular cAMP concentrations were measured at 0, 15, 30 and 60 min after 10 nM Ex-4 stimulation. Unpaired *t*-tests were performed to calculate statistical significance ($^{*}P < 0.05$ vs. 0 min, $^{**}P < 0.01$ vs. 0 min). (D) LNCaP cells were maintained in media supplemented with 10% FBS with or without 10 nM Ex-4 or 10 μM PKI_{14-22}. After 0, 24, 48, 72 and 96 h, the cells were harvested, and cell proliferation was analyzed by cell counting using a hemocytometer. Black circles with solid line = control (non-treated); black squares with dotted line = Ex-4 (10 nM); white circles with solid line = PKI_{14-22} (10 μM); white squares with dotted line = Ex-4 (10 nM) + PKI_{14-22} (10 μM). One-way ANOVA was performed to calculate statistical significance ($^{**}P < 0.01$ vs. control).

FIG. 5. Exendin-4 does not suppress androgen receptor activation. (A) LNCaP cells maintained in media supplemented with 10% charcoal-filtered FBS in 24-well plates were stimulated with 10^{-8} M DHT or vehicle for 24 h. RNA was isolated and quantitative RT-PCR was performed to examine *PSA* mRNA expression. (B) PSA protein secreted into the culture medium was assayed by EIA. LNCaP cells were

transiently transfected with (C) pGL3-MMTV or (D) pPSA-LUC, and maintained in media supplemented with 10% charcoal-filtered FBS with or without Ex-4 (0.1–10 nM) for 12 h followed by stimulation with 10^{-8} M DHT or solvent (ethanol) for 24 h. Luciferase activity was then measured. Unpaired *t*-tests were performed to calculate statistical significance [$^{**}P < 0.01$ vs. DHT(-); $^{\#\#}P < 0.05$ vs. DHT(+), Ex-4(-); †$P < 0.05$ vs. DHT(-), Ex-4(-)]. Transfection efficiency was adjusted by normalizing firefly luciferase activities to *Renilla* luciferase activities.

FIG. 6. Exendin-4 suppresses prostate cancer cell proliferation through inhibition of ERK-MAPK. (A) LNCaP cells were plated at a density of 3000 cells/well in 96-well plates in media supplemented with 10% FBS and incubated with Ex-4 (0–10 nM) for 24 h. BrdU solution was added during the last 4 h, and cells were harvested for measurement of DNA synthesis using a microplate reader at 450–620 nm. Mean data are expressed as a ratio of the control cell proliferation. Unpaired *t*-tests were performed to calculate statistical significance ($^{**}P < 0.01$ vs. control; $^{\#\#}P < 0.01$ vs. 0.1 nM Ex-4; ‡‡$P < 0.01$ vs. 1 nM Ex-4). (B) LNCaP cells were plated on glass coverslips in 6-well plates. After incubation with 10 nM Ex-4 or 1 unit/100 μl RQ1 DNase for 24 h, apoptotic cells were detected with TUNEL staining. Images shown are representative of

triplicate independent experiments. (C) LNCaP cells maintained in media with 10% FBS were stimulated with 10 nM Ex-4 or saline for 15 min. Cell lysates were harvested and subjected to western blotting to assess phosphorylated ERK-MAPK and ERK-MAPK expression. Phosphorylated ERK-MAPK/ERK-MAPK protein levels were quantified by densitometry. Data were calculated from triplicate independent experiments and are shown as a ratio of the control. Unpaired *t*-tests were performed to calculate statistical significance ($^{*}P < 0.05$ vs. control). (D) LNCaP cells maintained in media with 10% FBS were treated with 10 μM PKI_{14-22} or vehicle for 30 min before the addition of 10 nM Ex-4 for 15 min. Cell lysates were harvested and subjected to western blotting to assess phosphorylated ERK-MAPK and ERK-MAPK. Phosphorylated ERK-MAPK/ERK-MAPK protein levels were quantified by densitometry. Data were calculated from four independent experiments and are shown as a ratio of the PKI(-), Ex-4(-). Unpaired *t*-tests were performed to calculate significance [$^{*}P < 0.05$ vs. PKI(-),Ex-4(-); $^{\#}P < 0.05$ vs. PKI(+), Ex-4(+)]. (E) LNCaP cells were maintained in media supplemented with 10% FBS with or without Ex-4 (10 nM) and 10 μM PD98059. After 0, 24, 48, 72 and 96 h, the cells were harvested and cell proliferation was analyzed by cell counting using a hemocytometer. Black circles with solid line = control (non-treated); black squares with dotted line = Ex-4 (10 nM); white

circles with solid line = PD98059 (10 nM); white squares with dotted line = Ex-4 (10 nM) + PD98059 (10 μM). One-way ANOVA was performed to calculate statistical significance ($^{**}P < 0.01$ vs. control, $^{\#\#}P < 0.01$ vs. Ex-4 or PD98059).

FIG. 7. Exendin-4 attenuates prostate cancer growth in vivo. (A) Athymic CAnN.Cg-*Foxn1nu*/CrlCrlj mice (aged 6 weeks) were transplanted with 1×10^6 LNCaP cells (passages 4–8) and treated with either vehicle (n = 7), high dose Ex-4 (24 nmol/kg body weight/day; n = 7) or low dose Ex-4 (300 pmol/kg body weight/day; n = 8). Tumors were imaged at 12 weeks of age. (B) Tumor volume was calculated with the modified ellipsoid formula. One-way ANOVA was performed to calculate statistical significance ($^{*}P < 0.05$ vs. control). Sections (5 μm) were subjected to immunohistochemistry for (C) P504S, (E) Ki67, (G) phosphorylated ERK-MAPK, or (I) P504S and GLP-1R, and counterstained with DAPI. Magnification, ×400. (D) P504S, (F) Ki67, (H) phosphorylated ERK-MAPK, or (I) P504S and GLP-1R-positive cells were quantified by analyzing the fraction of stained cells in the tumor relative to the total number of nuclei. Values are expressed as a percentage of positive cells. Unpaired *t*-tests were performed to calculate statistical significance ($^{**}P < 0.01$ vs. control; $^{\#\#}P < 0.01$ vs. low dose Ex-4; $^{\ddagger\ddagger}P < 0.01$ vs. 0.1 nM Ex-4).

Table 1. Characteristics of Ex-4-treated athymic mice following transplantation of LNCaP cells.

	Control	Ex-4 (300 pmol/kg/day)	Ex-4 (24 nmol/kg/day)
Body weight (g)	22.6 ± 1.2	23.9 ± 0.9	21.9 ± 1.0
Plasma glucose (mg/dl)	128.6 ± 6.2	127.4 ± 11.4	135.8 ± 7.8
Plasma PSA (ng/ml)	6.2 ± 1.1	4.3 ± 0.8	3.9 ± 0.8

DAPI

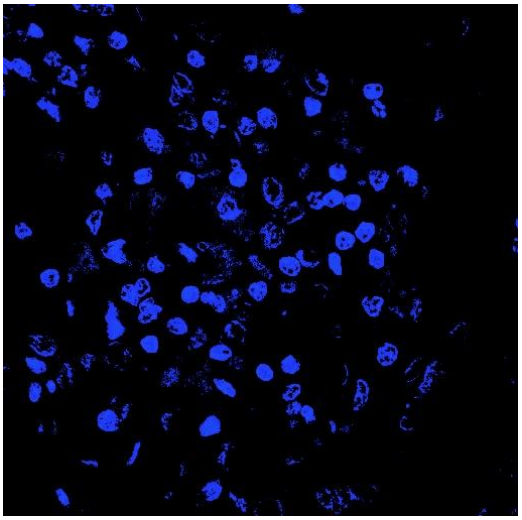

P504S

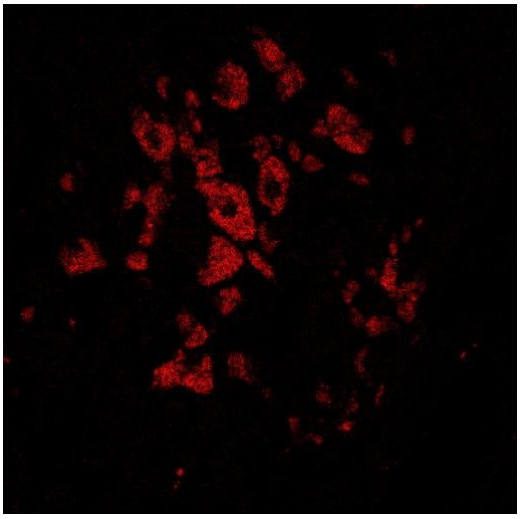

GLP-1R

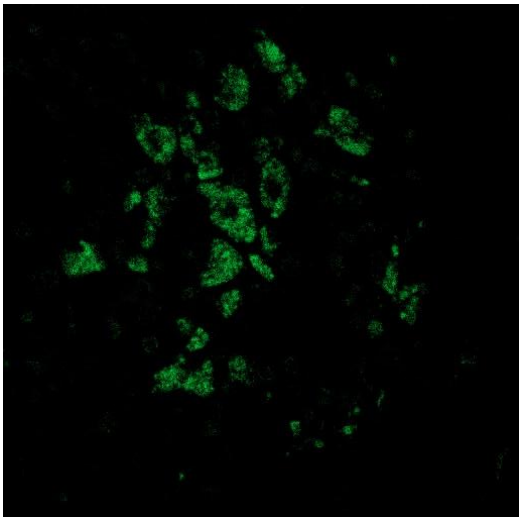

Merge

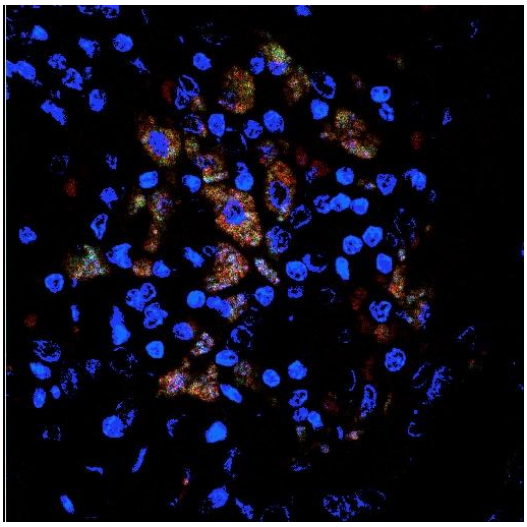

Figure 2

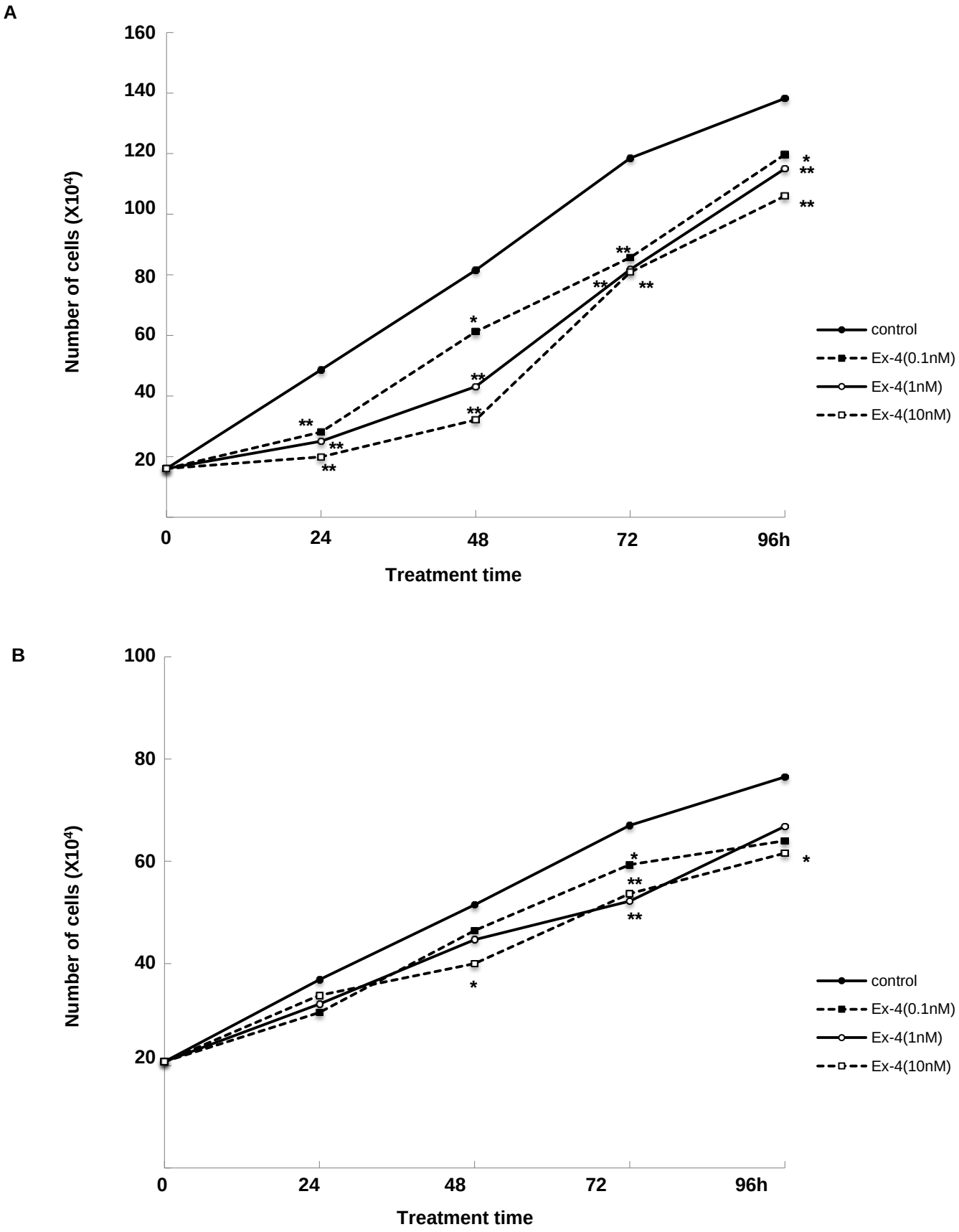
A
160
140
120
100
80
60
40
20
Number of cells (X10⁴)
0
24
48
72
96h
Treatment time
control
Ex-4(0.1nM)
Ex-4(1nM)
Ex-4(10nM)
B
100
80
60
40
20
Number of cells (X10⁴)
0
24
48
72
96h
Treatment time
control
Ex-4(0.1nM)
Ex-4(1nM)
Ex-4(10nM)

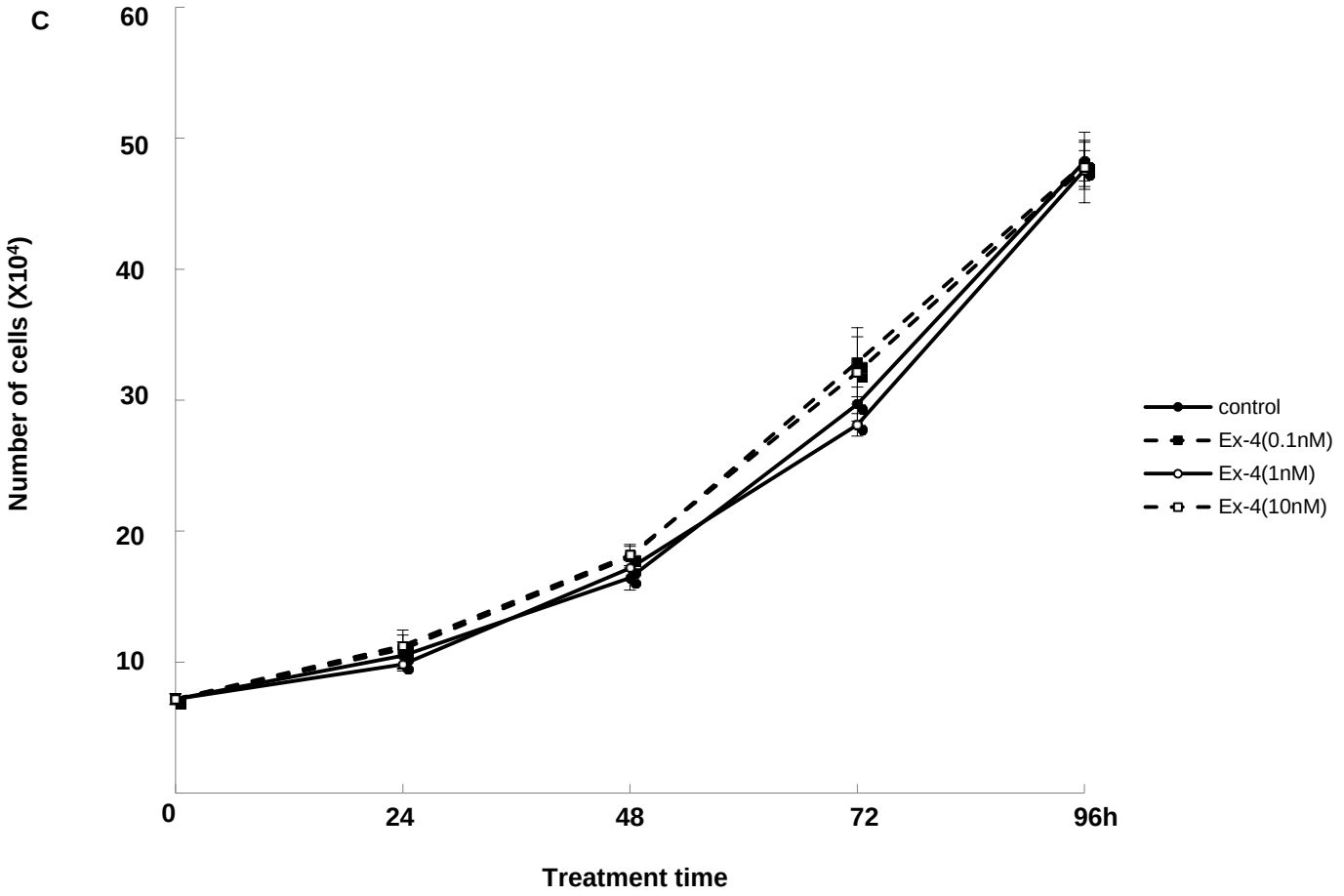
C
60
50
40
30
20
10
Number of cells (X10⁴)
0
24
48
72
96h
Treatment time
control
Ex-4(0.1nM)
Ex-4(1nM)
Ex-4(10nM)

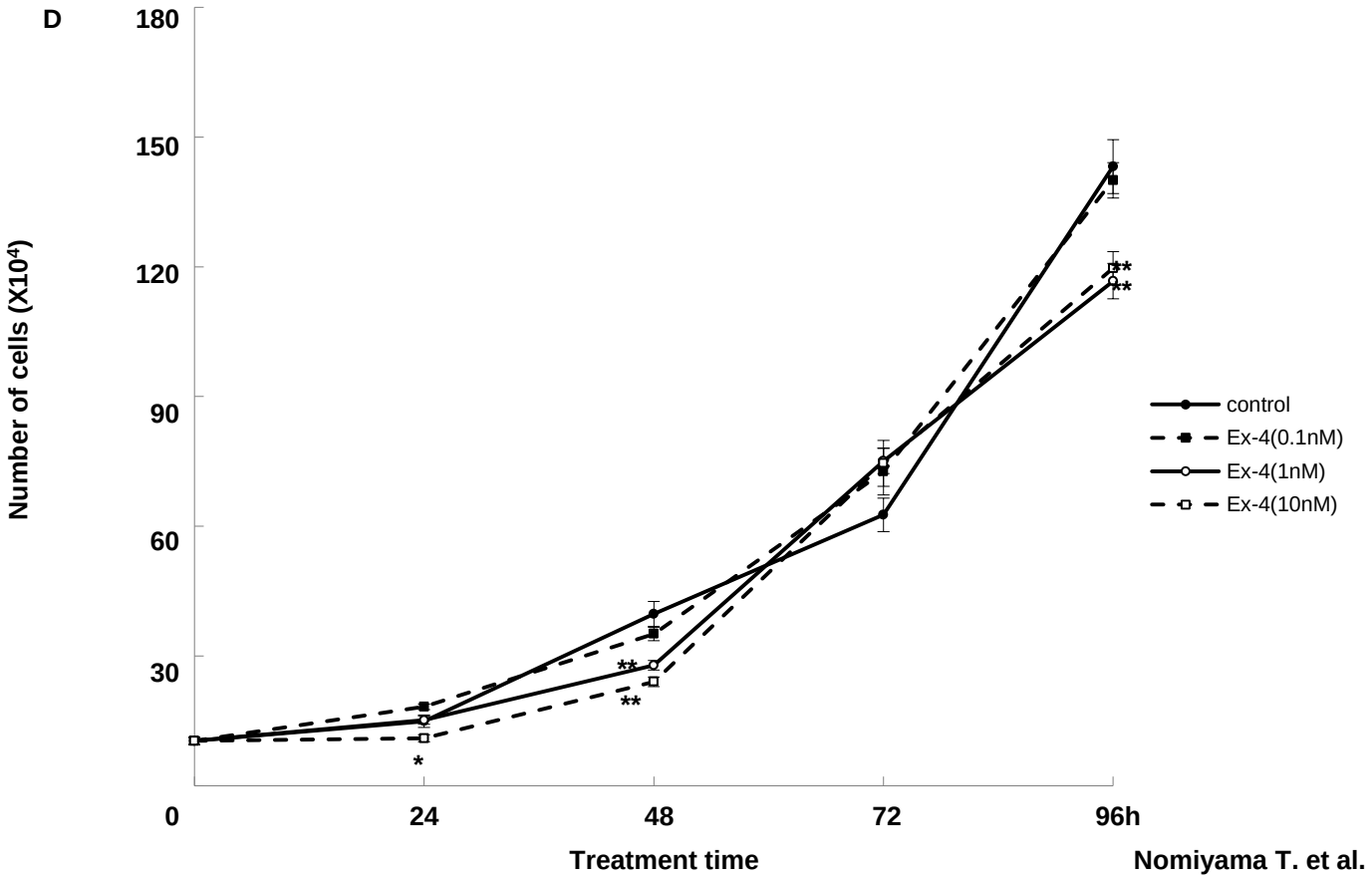
D
180
150
120
90
60
30
Number of cells (X10⁴)
0
24
48
72
96h
Treatment time
*
**
**
**
**
control
Ex-4(0.1nM)
Ex-4(1nM)
Ex-4(10nM)

Figure 3

A

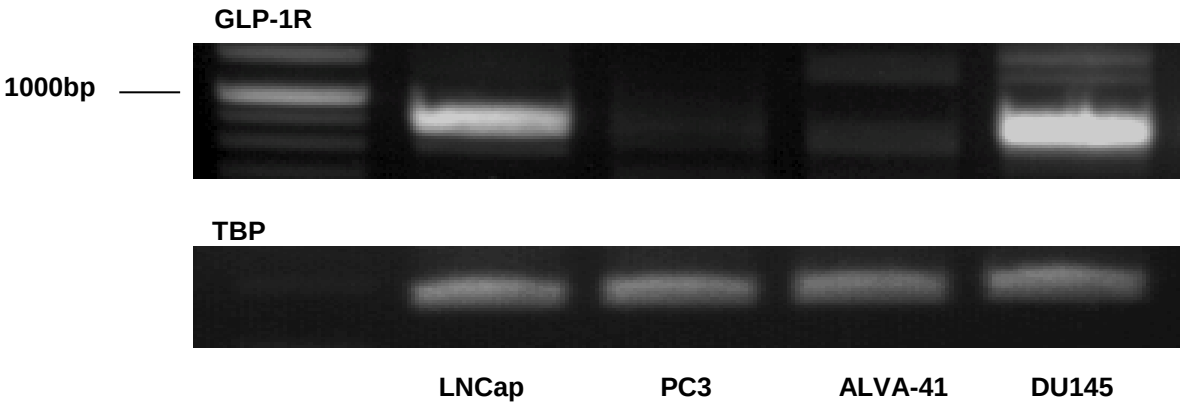
GLP-1R
1000bp
TBP
LNCap
PC3
ALVA-41
DU145

B

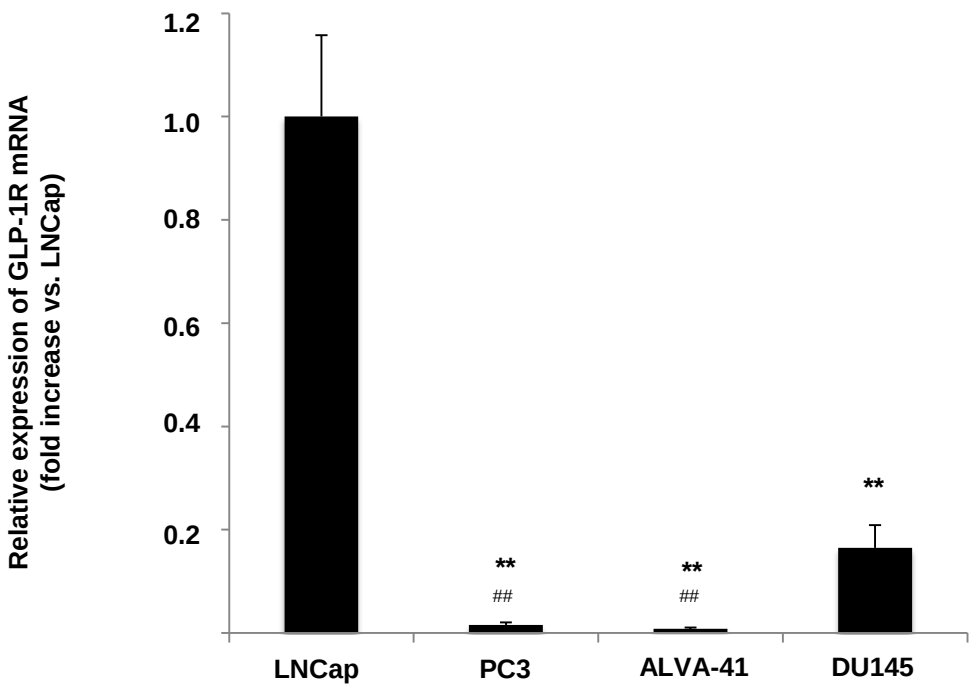
Relative expression of GLP-1R mRNA
(fold increase vs. LNCap)
1.2
1.0
0.8
0.6
0.4
0.2
**
##
**
##
**
LNCap
PC3
ALVA-41
DU145

C

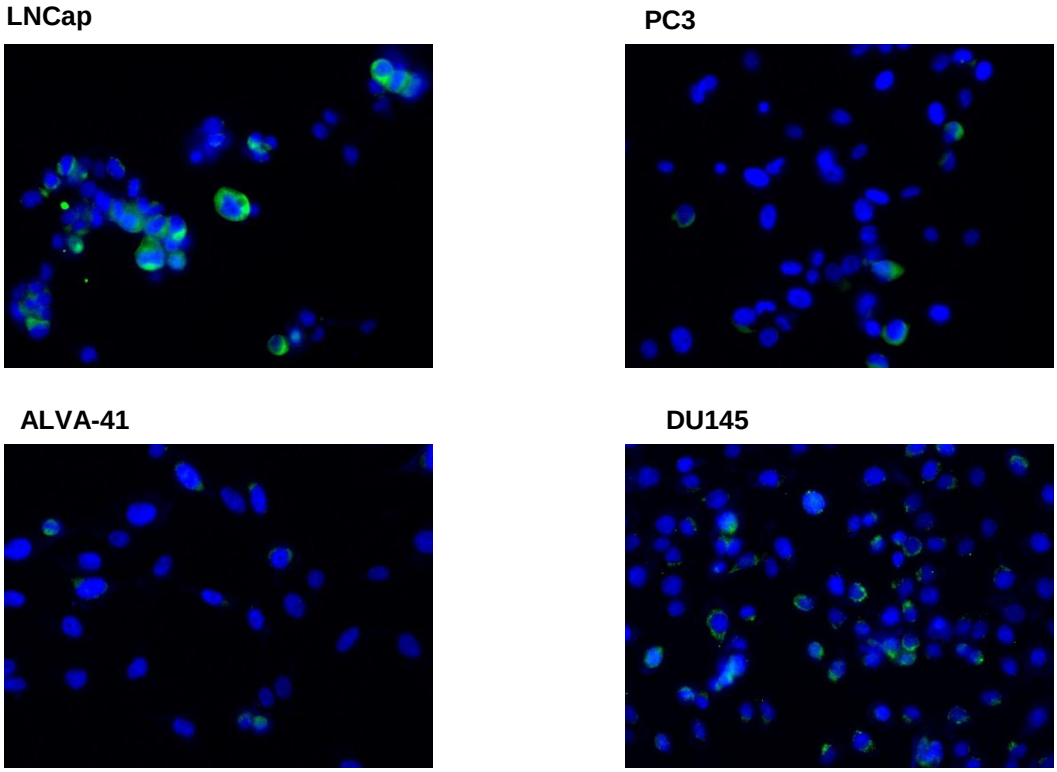
LNCap
PC3
ALVA-41
DU145

D

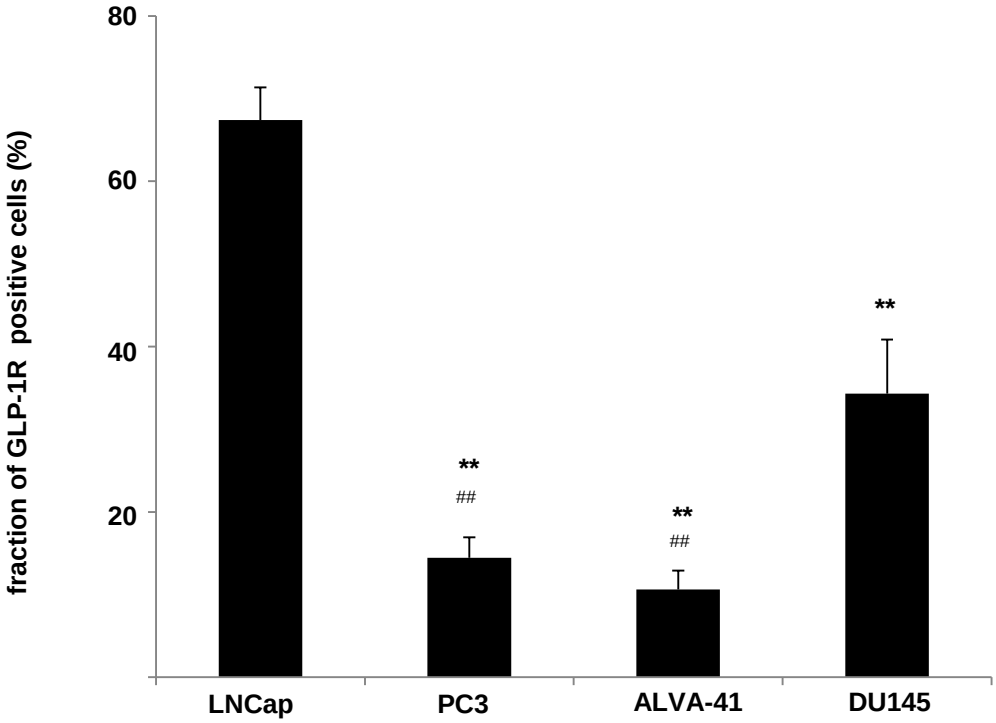
fraction of GLP-1R positive cells (%)
80
60
40
20
**
##
**
##
**
LNCap
PC3
ALVA-41
DU145

Figure 4

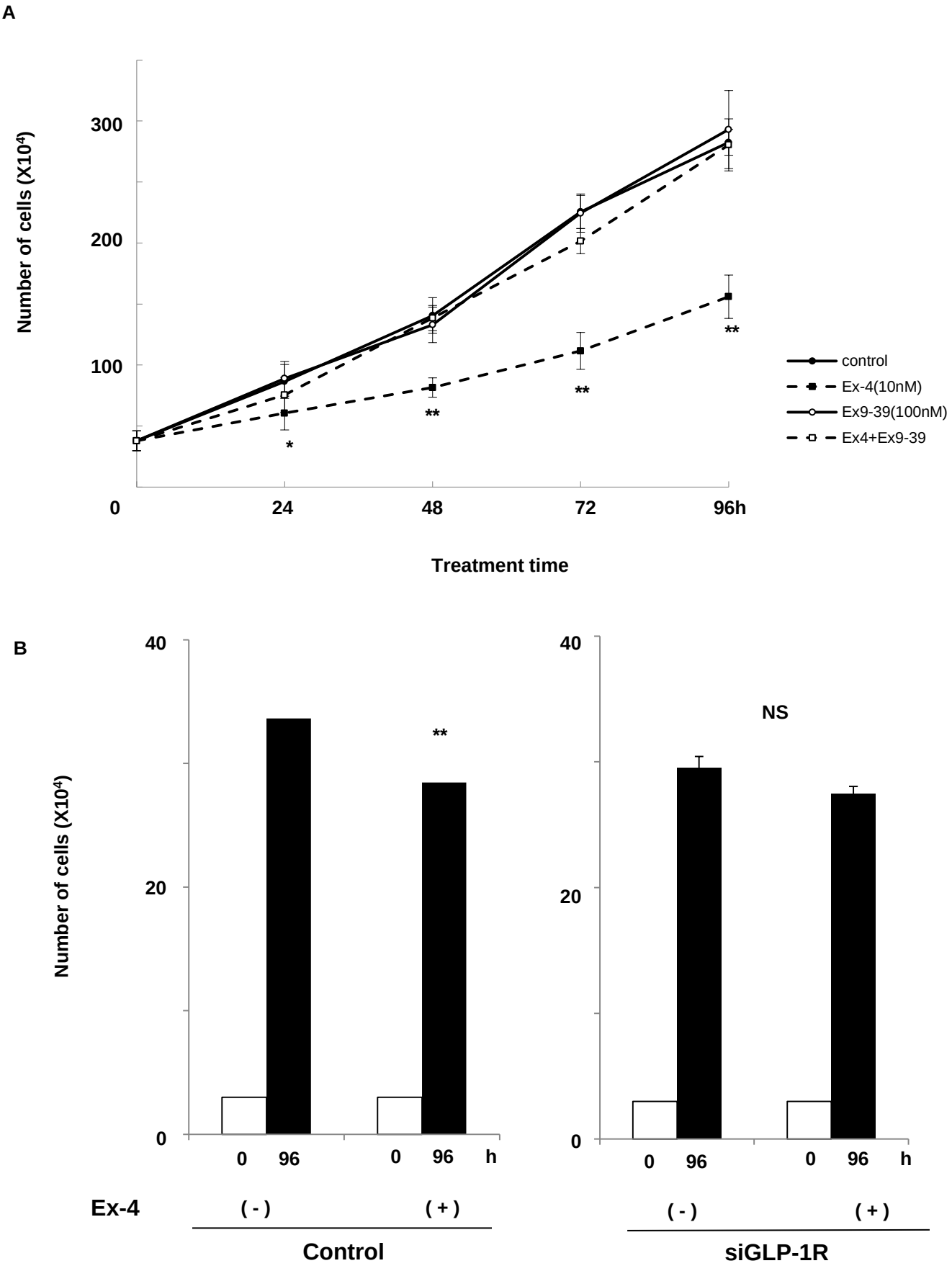
A
Number of cells (X10⁴)
300
200
100
0
24
48
72
96h
Treatment time
control
Ex-4(10nM)
Ex9-39(100nM)
Ex4+Ex9-39
*
**
**
**
B
Number of cells (X10⁴)
40
20
0
**
NS
0
96
h
Ex-4
(-)
(+)
Control
siGLP-1R

C

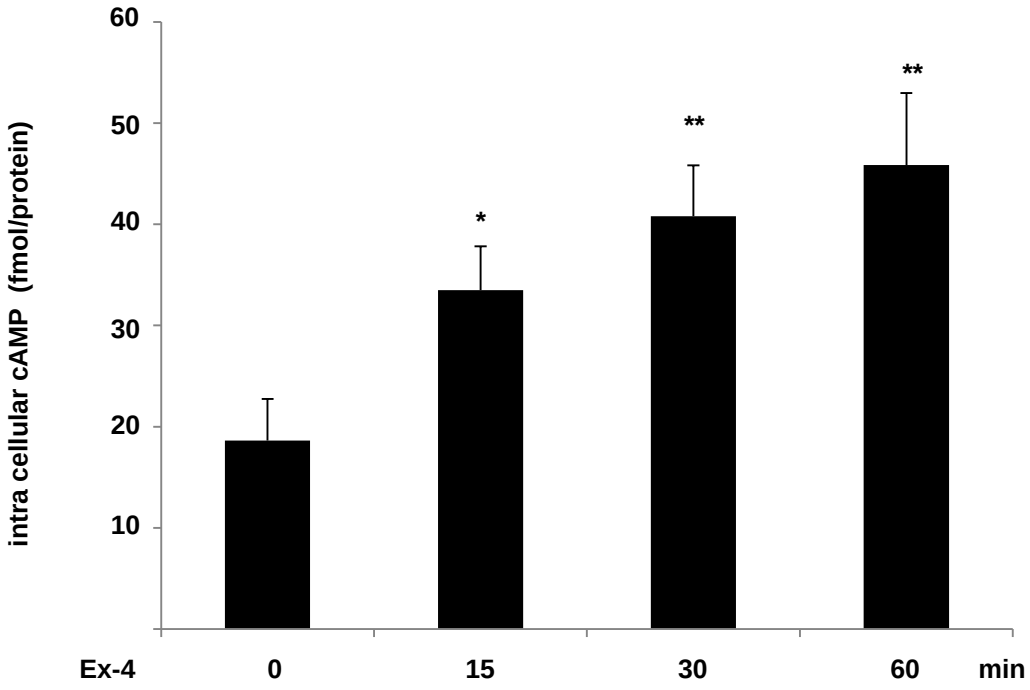
intra cellular cAMP (fmol/protein)
60
50
40
30
20
10
*
**
**
Ex-4
0
15
30
60
min

D

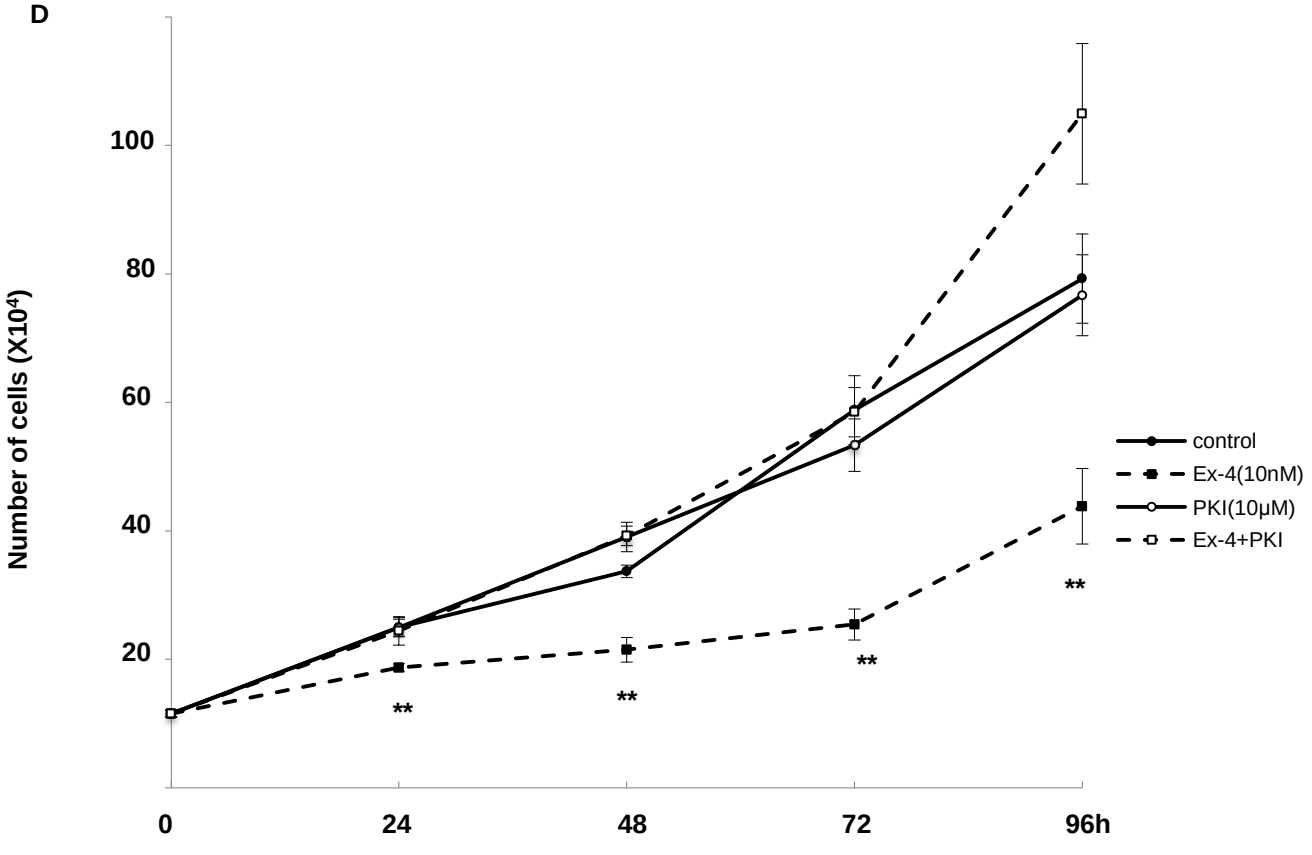
Number of cells (X10⁴)
100
80
60
40
20
**
**
**
**
0
24
48
72
96h
Treatment time
control
Ex-4(10nM)
PKI(10μM)
Ex-4+PKI

Figure 5

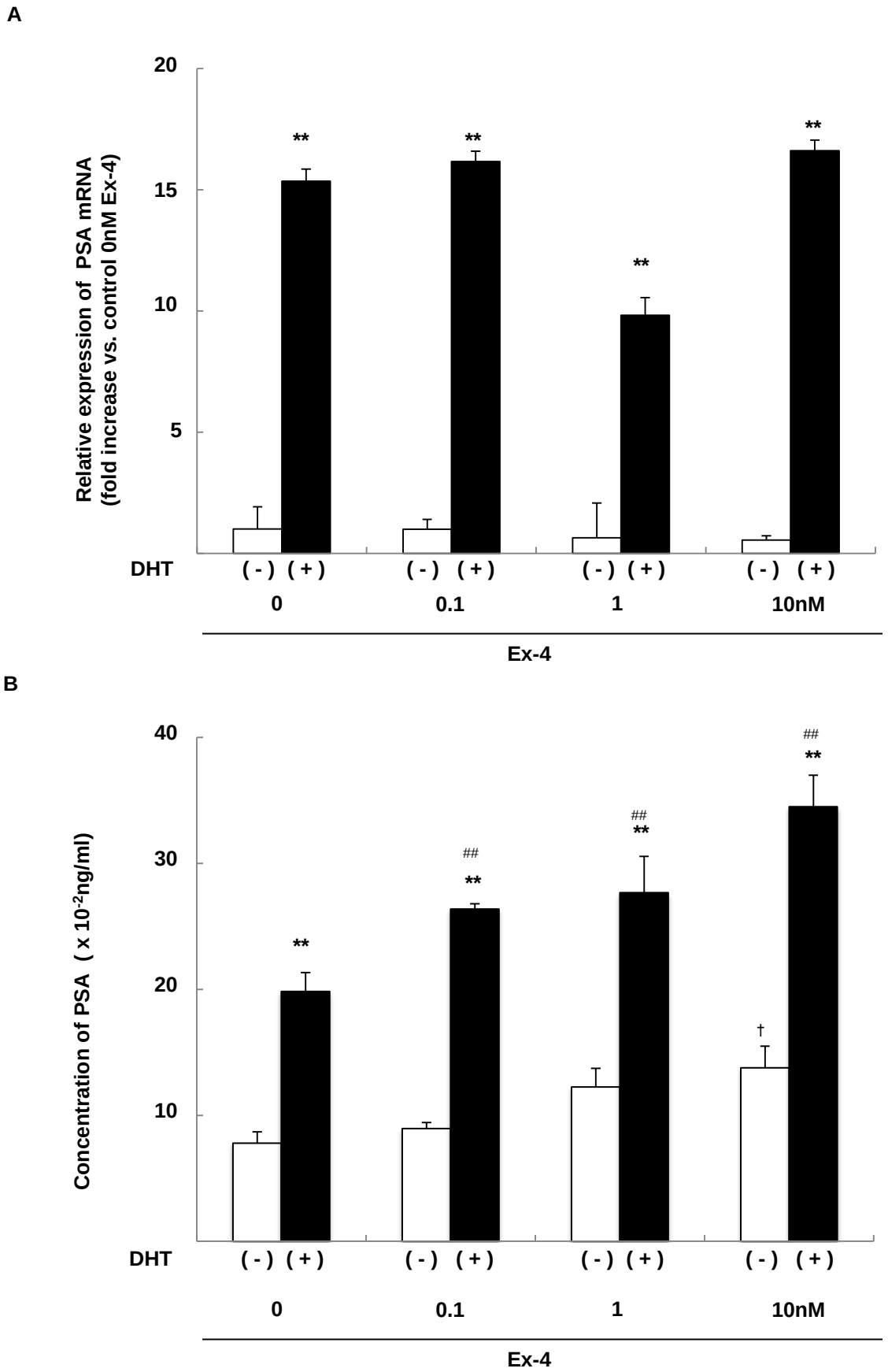
A
Relative expression of PSA mRNA
(fold increase vs. control 0nM Ex-4)
20
15
10
5
**
DHT
(-) (+)
0
0.1
1
10nM
Ex-4
B
Concentration of PSA (x 10-2ng/ml)
40
30
20
10
##
†

C

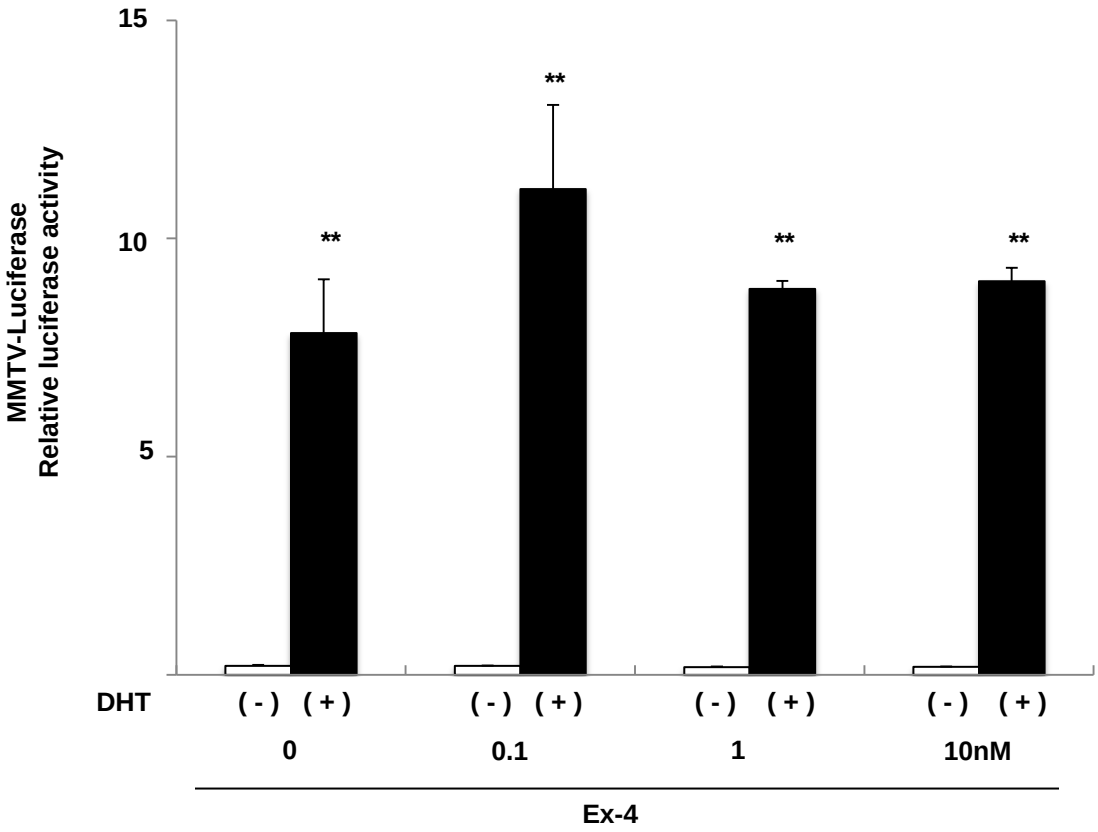
MMTV-Luciferase
Relative luciferase activity
15
10
5
**
**
**
**
DHT
(-) (+)
(-) (+)
(-) (+)
(-) (+)
0
0.1
1
10nM
Ex-4

D

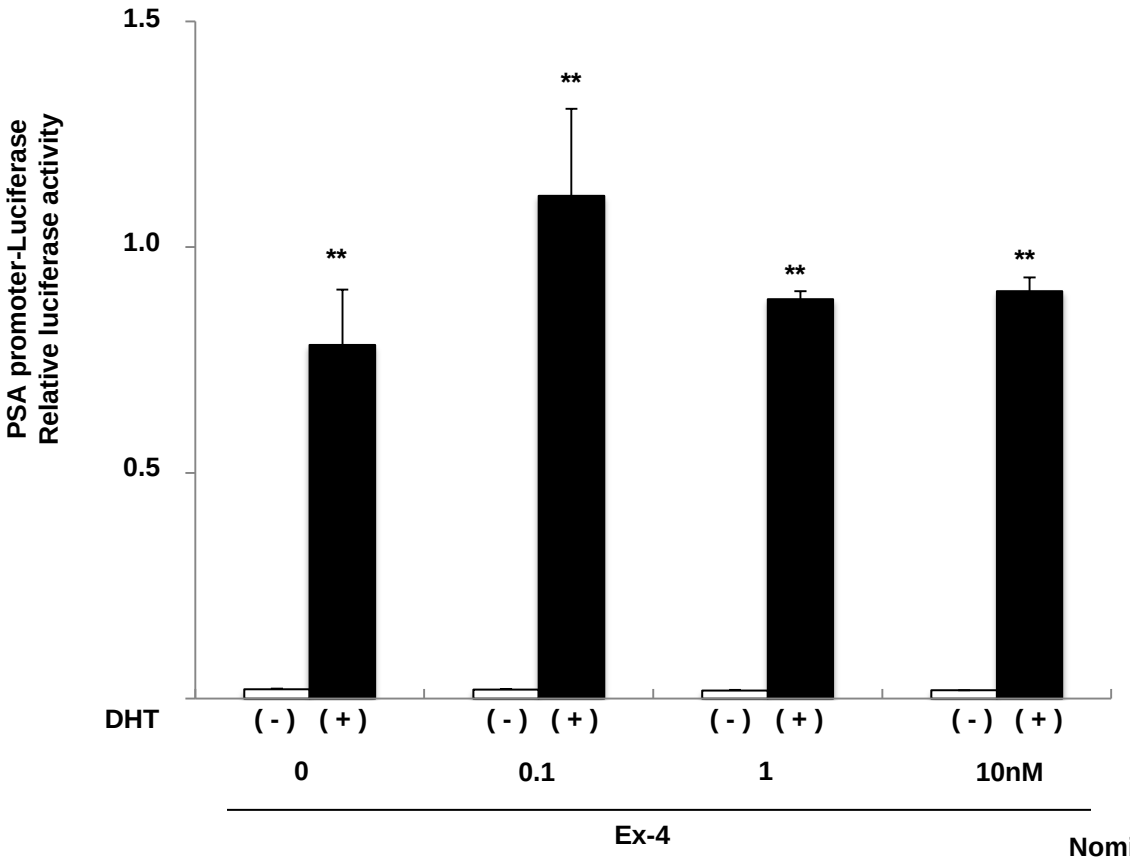
PSA promoter-Luciferase
Relative luciferase activity
1.5
1.0
0.5
**
**
**
**
DHT
(-) (+)
(-) (+)
(-) (+)
(-) (+)
0
0.1
1
10nM
Ex-4

Figure 6

A

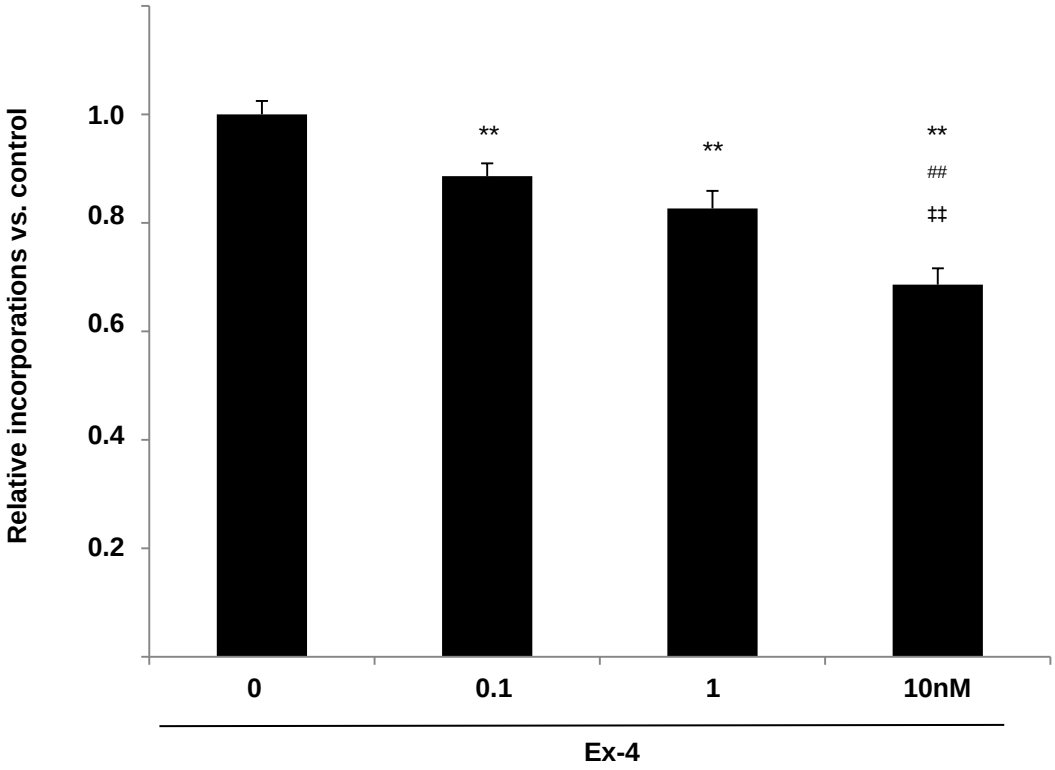
Relative incorporations vs. control
1.0
0.8
0.6
0.4
0.2
**
**
**
##
‡‡
0
0.1
1
10nM
Ex-4

B

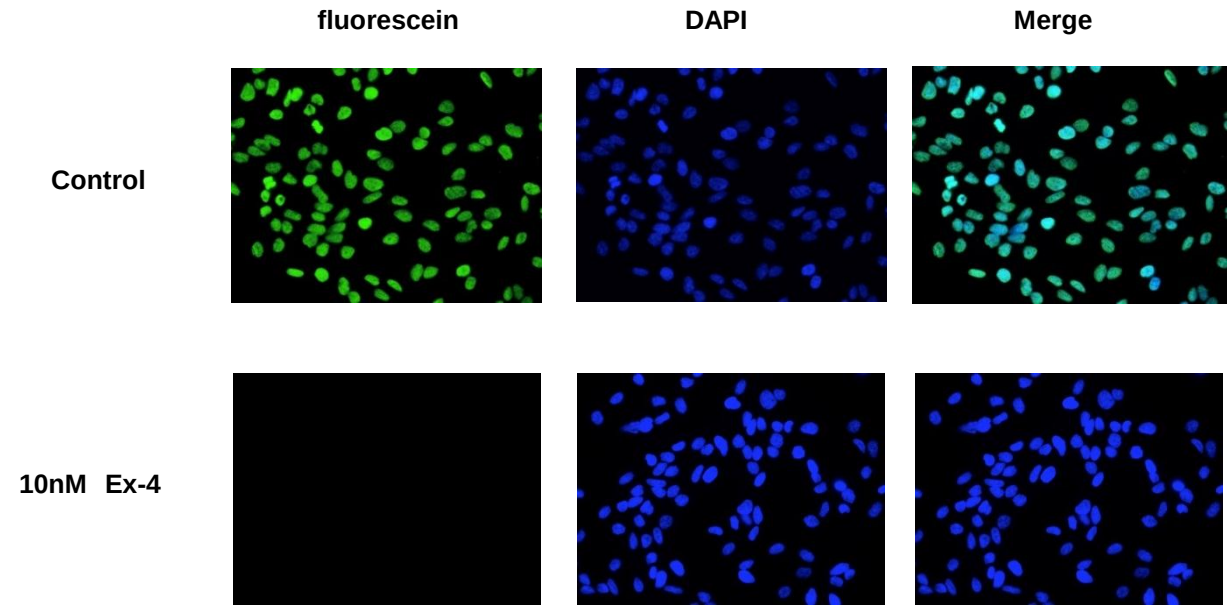
fluorescein
DAPI
Merge
Control
10nM Ex-4

C

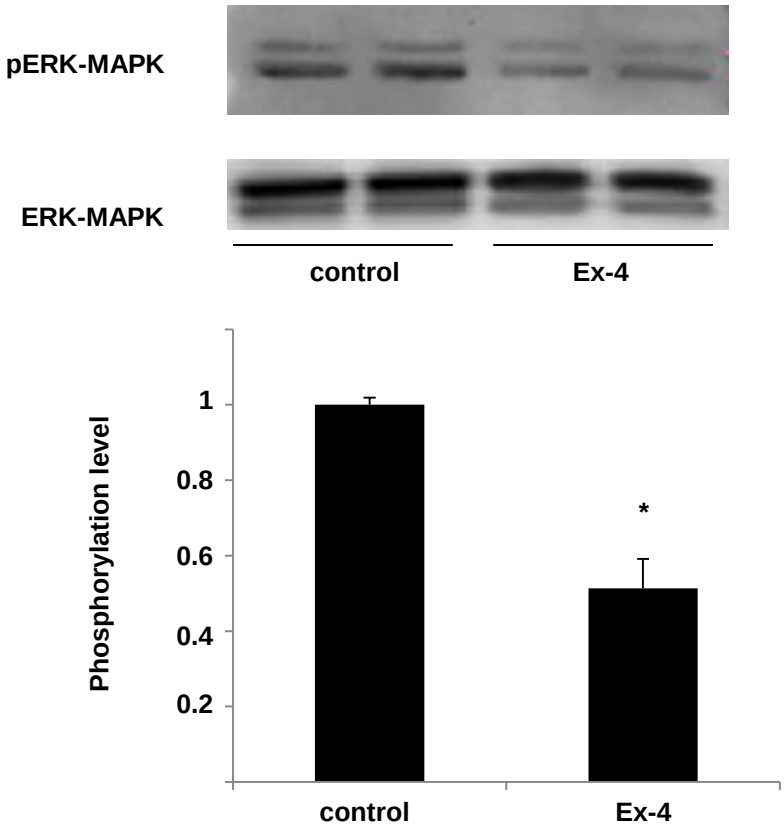
pERK-MAPK
ERK-MAPK
control
Ex-4
Phosphorylation level
1
0.8
0.6
0.4
0.2
*
control
Ex-4

D

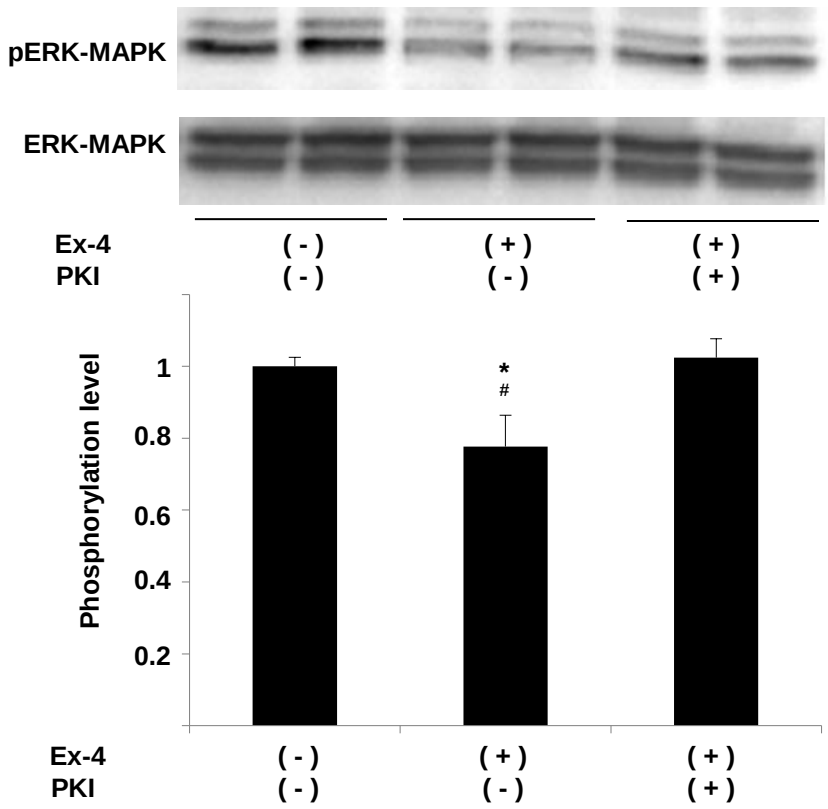
pERK-MAPK
ERK-MAPK
Ex-4
PKI
(-)
(-)
(+)
(-)
(+)
(+)
Phosphorylation level
1
0.8
0.6
0.4
0.2
*
#
Ex-4
PKI
(-)
(-)
(+)
(-)
(+)
(+)

E

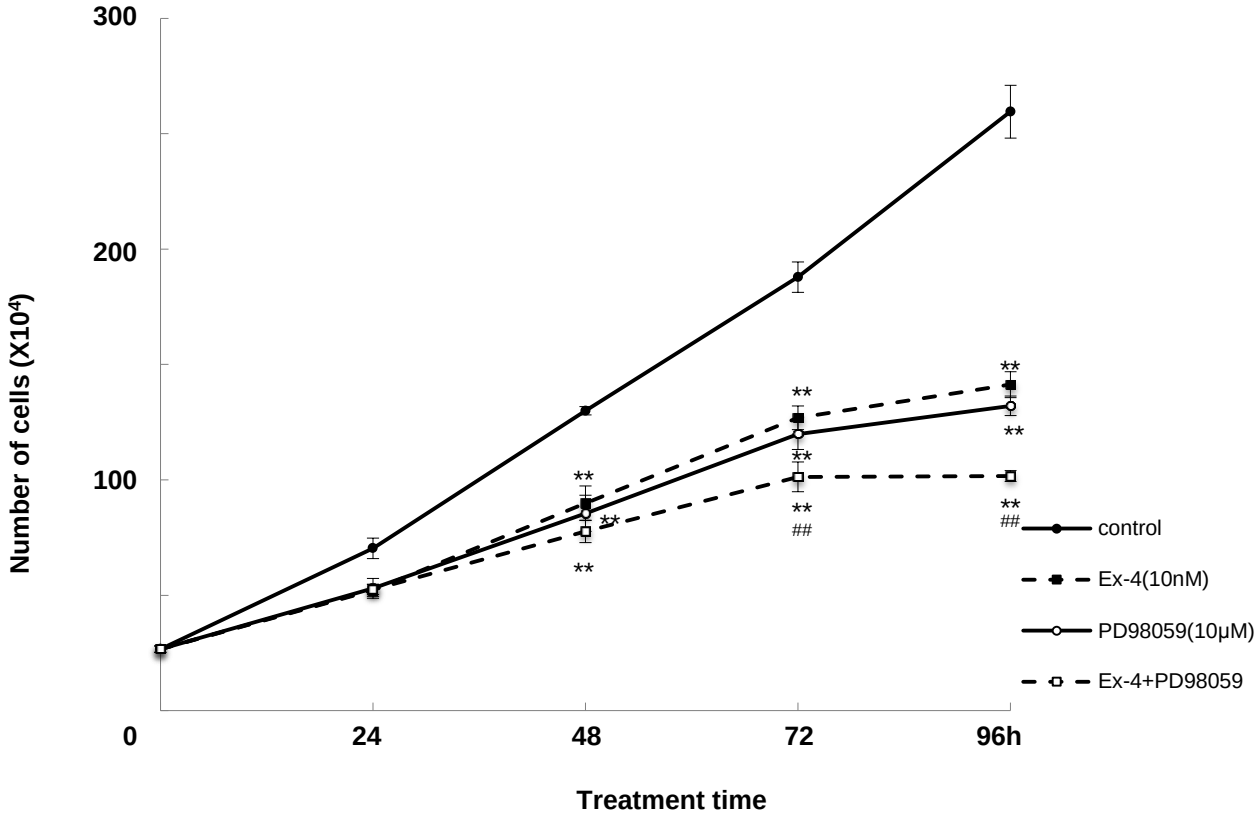
300
200
100
0
Number of cells (X10⁴)
24
48
72
96h
Treatment time
control
Ex-4(10nM)
PD98059(10μM)
Ex-4+PD98059
**
##

A

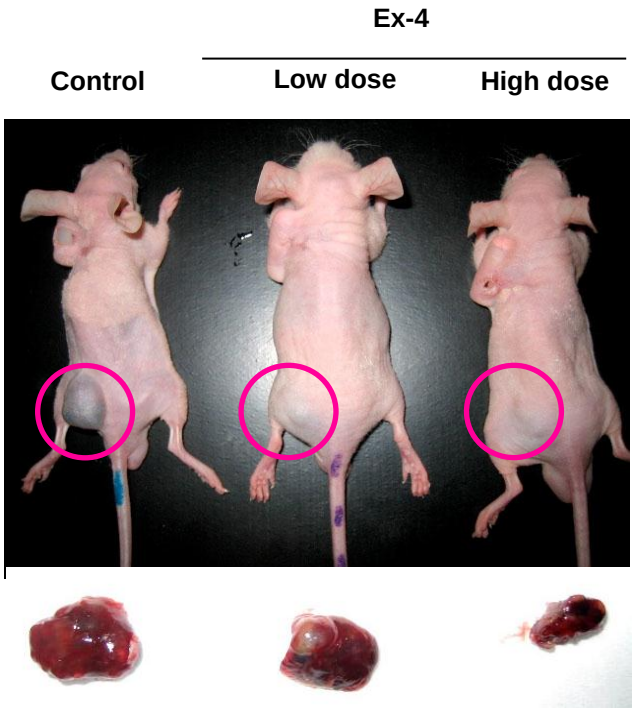
Ex-4
Control
Low dose
High dose

B

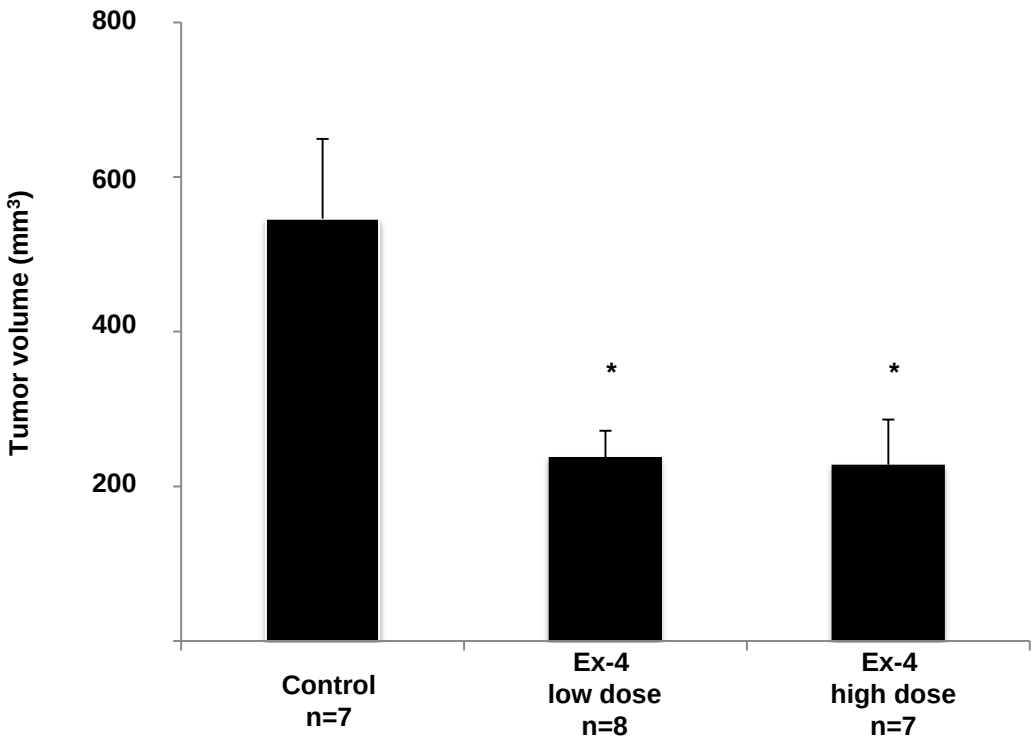
800
600
400
200
Tumor volume (mm3)
*
*
Control
n=7
Ex-4
low dose
n=8
Ex-4
high dose
n=7

C

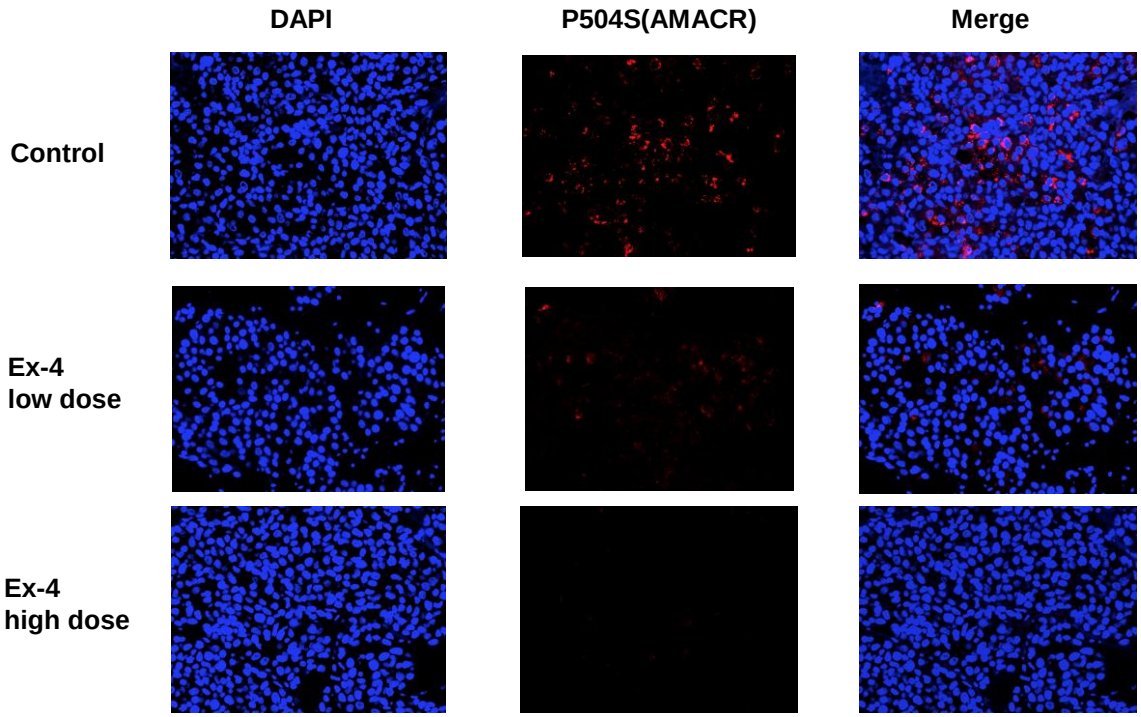
DAPI
P504S(AMACR)
Merge
Control
Ex-4
low dose
Ex-4
high dose

D

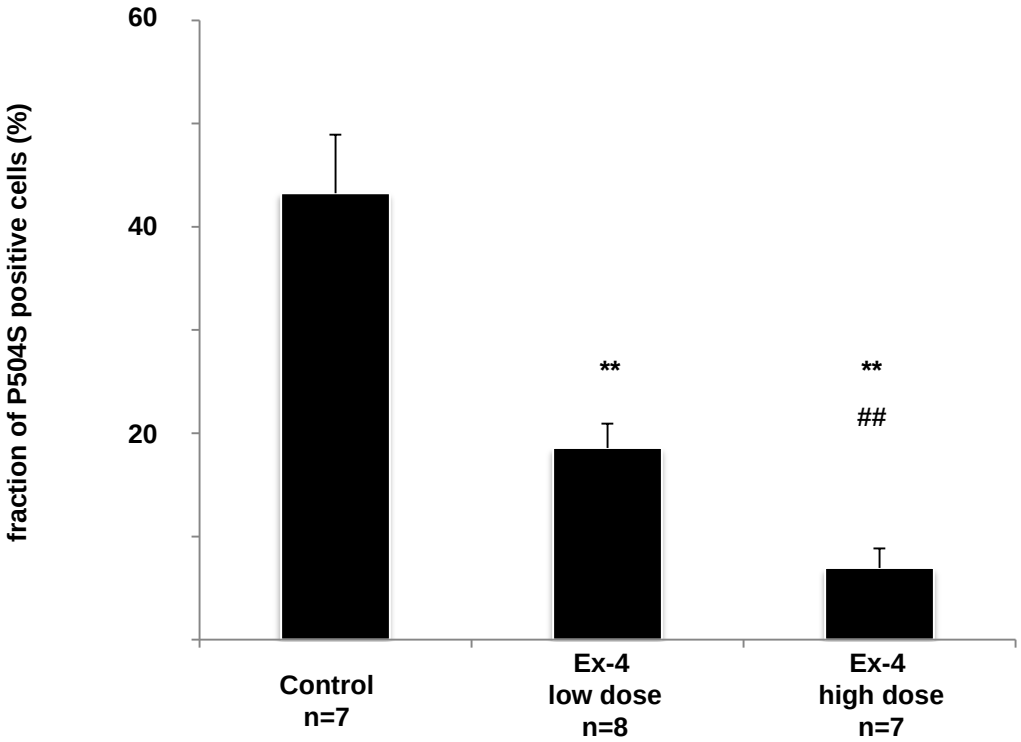
60
40
20
fraction of P504S positive cells (%)
**
**
##
Control
n=7
Ex-4
low dose
n=8
Ex-4
high dose
n=7

E

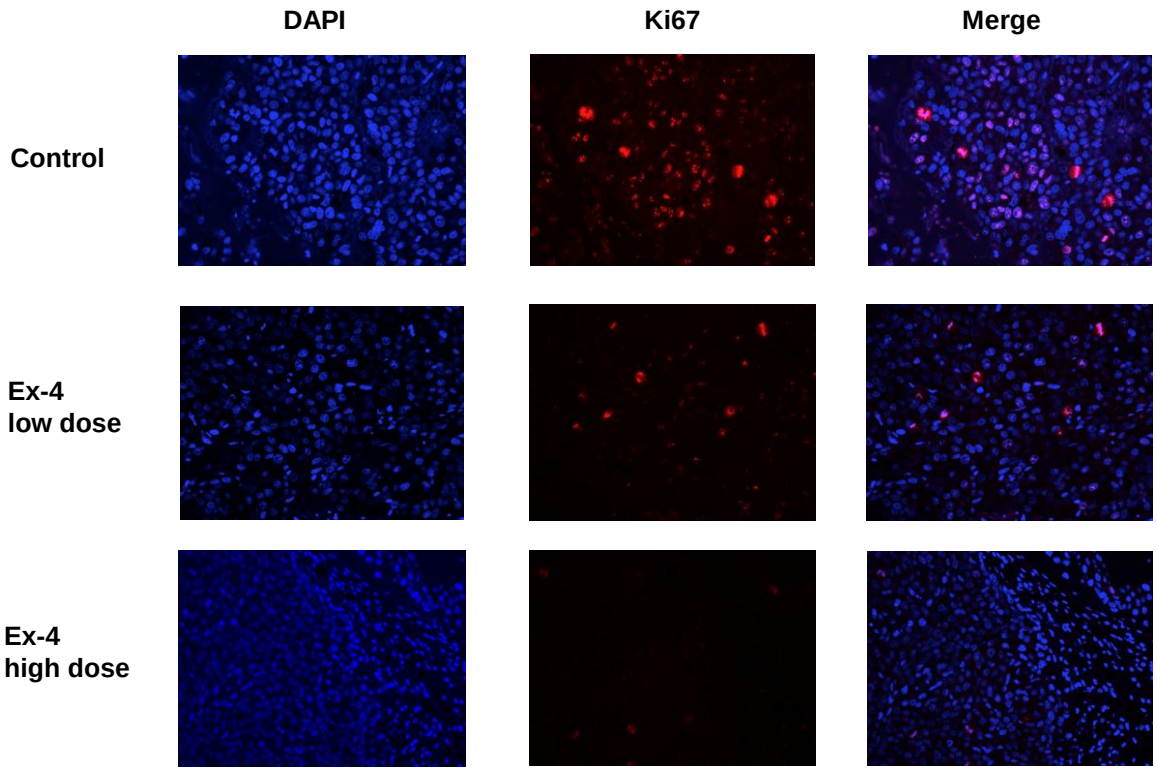
DAPI
Ki67
Merge
Control
Ex-4
low dose
Ex-4
high dose

F

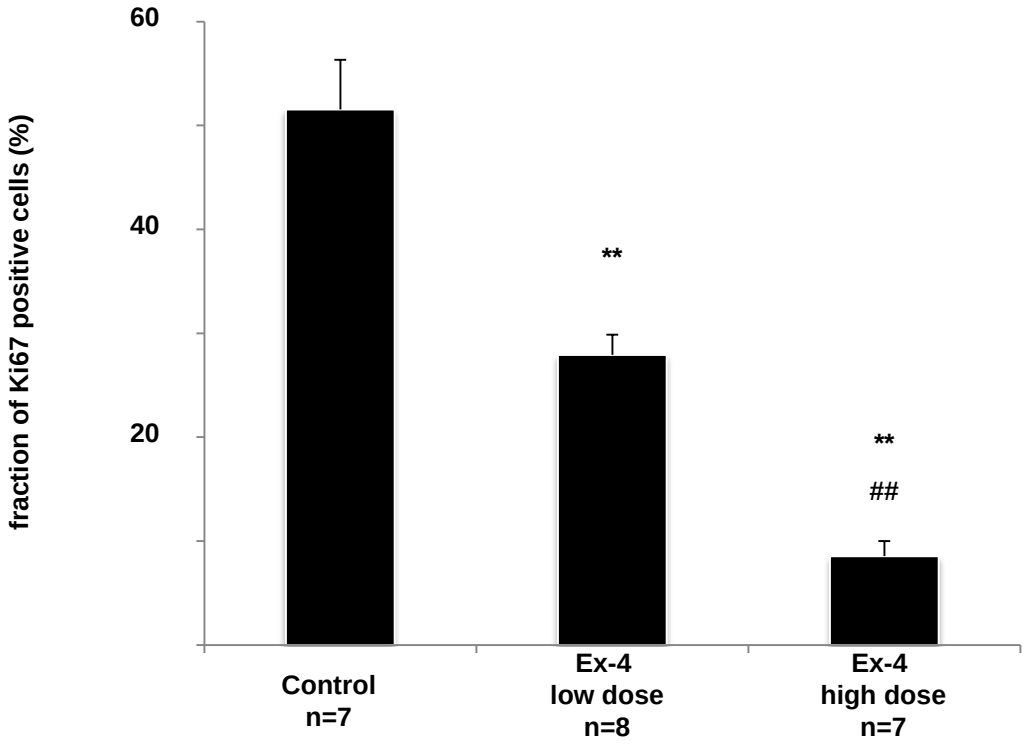
60
40
20
fraction of Ki67 positive cells (%)
**
**
##
Control
n=7
Ex-4
low dose
n=8
Ex-4
high dose
n=7

G

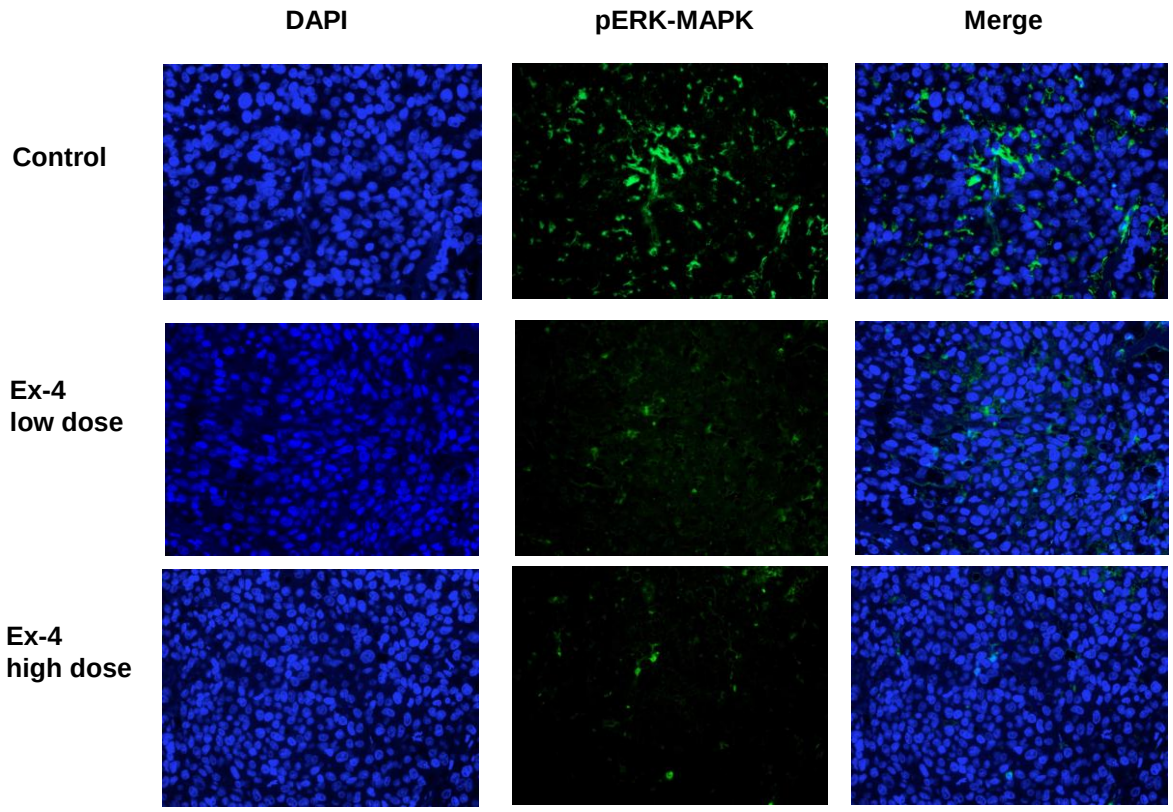
DAPI
pERK-MAPK
Merge
Control
Ex-4
low dose
Ex-4
high dose

H

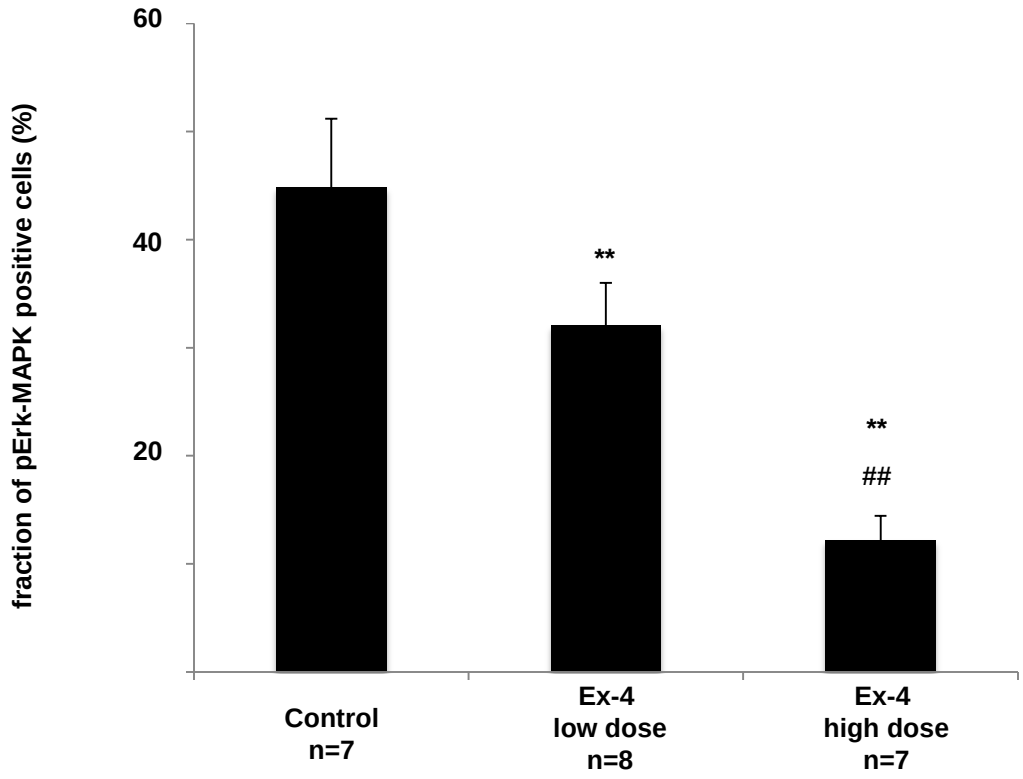
60
40
20
fraction of pErk-MAPK positive cells (%)
**
**
##
Control
n=7
Ex-4
low dose
n=8
Ex-4
high dose
n=7

I

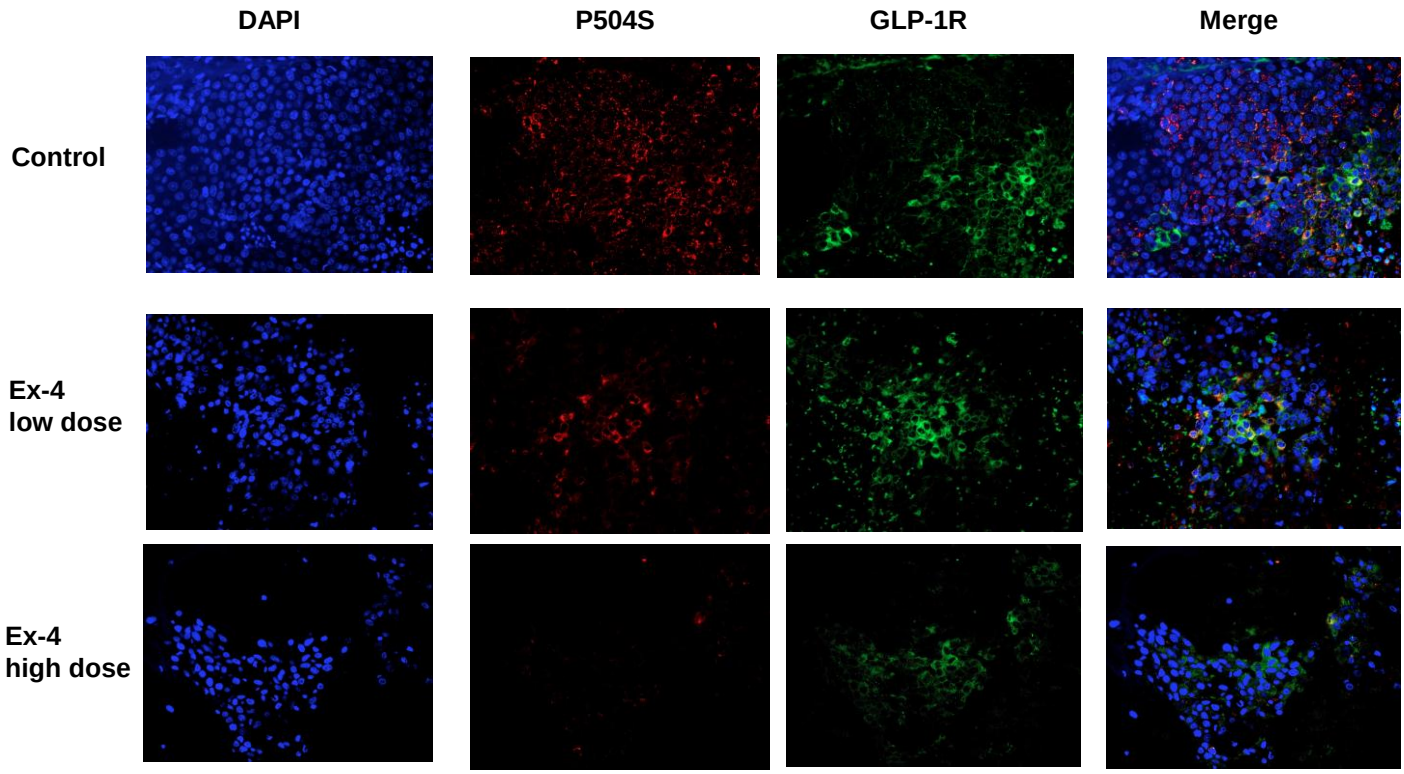
DAPI
P504S
GLP-1R
Merge
Control
Ex-4
low dose
Ex-4
high dose

J

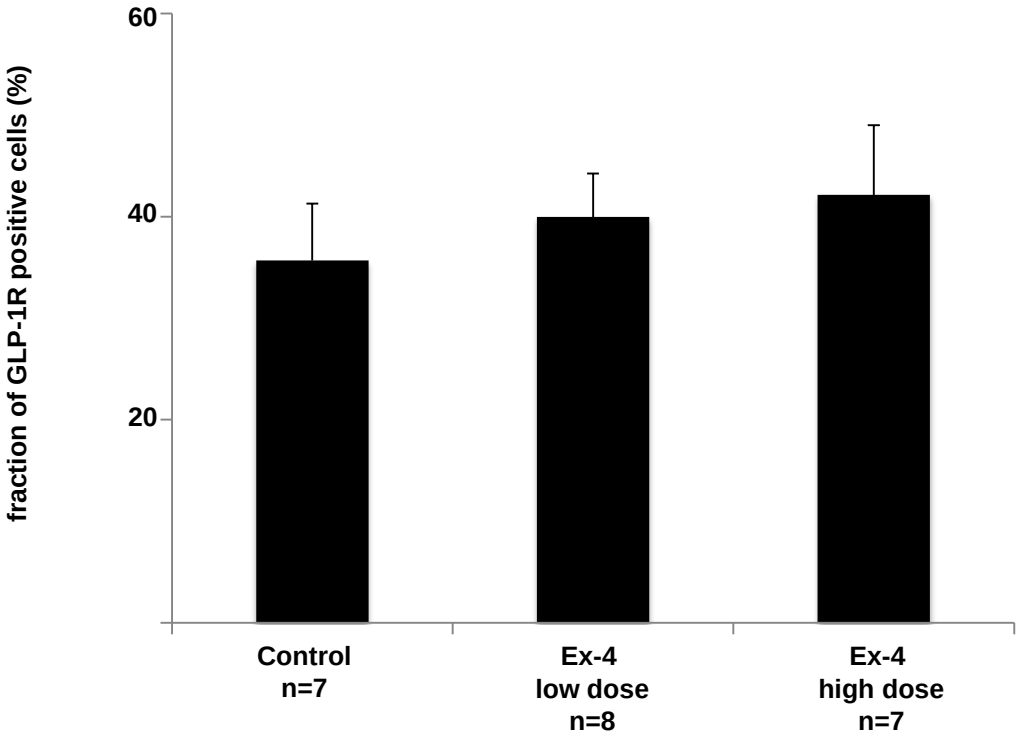
fraction of GLP-1R positive cells (%)
60
40
20
Control
n=7
Ex-4
low dose
n=8
Ex-4
high dose
n=7

Supplemental Fig. 1

Evaluation of different antibodies against GLP-1R. COS-7 cells transiently transfected with either an expression vector for GLP-1R (hGLP1R-pFN21AB7198, Kazusa DNA Research Institute, Promega) or a control vector (pcDNA3.1; Promega) were used to test the specificity of two different anti-GLP-1R antibodies, NBP1-97308 (Novus Biologicals) and ab39072 (Abcam), by immunofluorescent labeling. Sections were counterstained with DAPI and visualized by confocal microscopy.

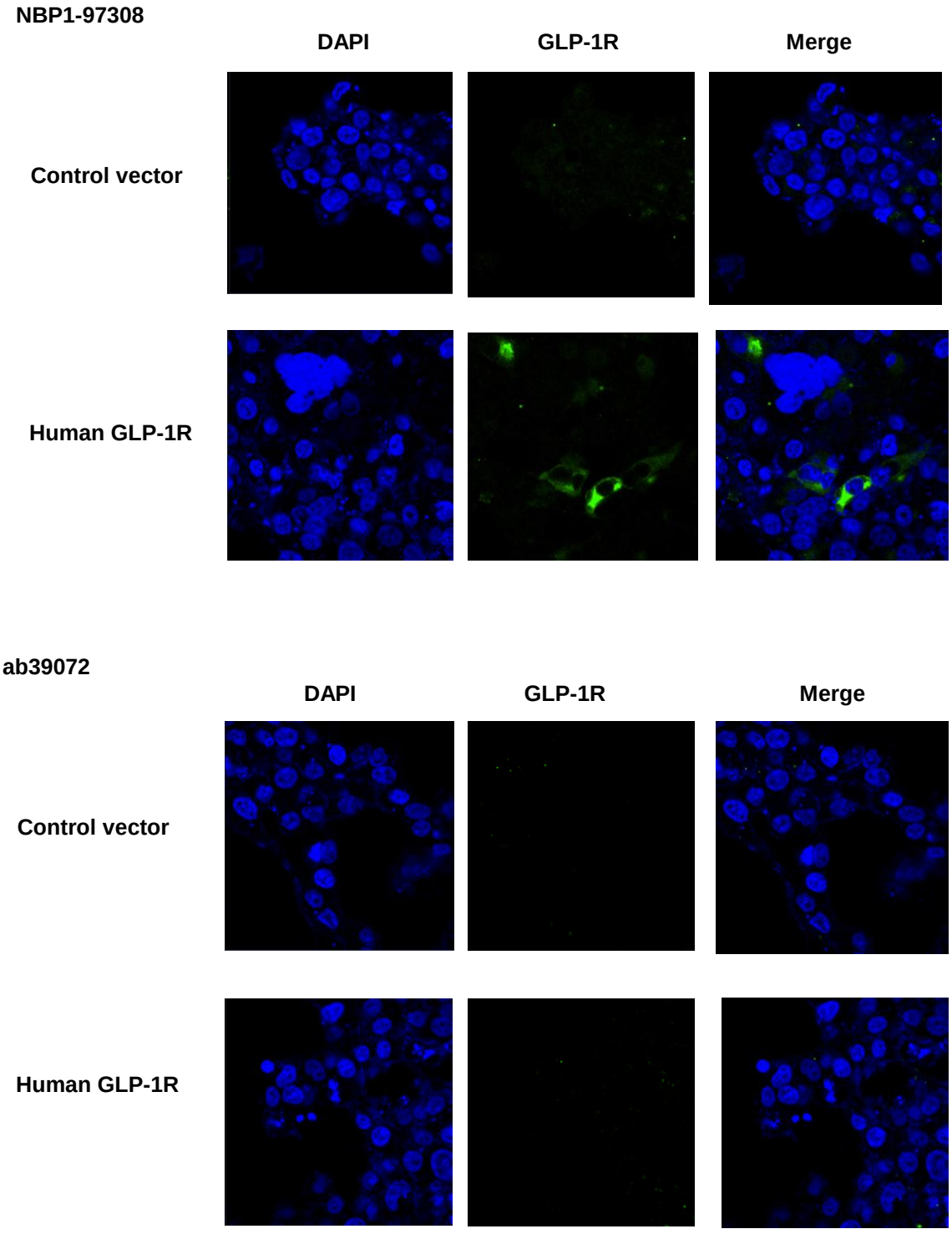

Validation of *GLP-1R* siRNA. *GLP-1R* mRNA expression in LNCaP cells transiently transfected with siRNA directed against *GLP-1R* (*GLP-1R* RNAi) or control primers was examined by RT-PCR. *TBP* mRNA levels were determined as an input control. (A) RT-PCR of the 890 bp coding sequence of human *GLP-1R* was performed as previously reported (26). (B) Quantitative RT-PCR of human *GLP-1R* was performed as described in RESEARCH DESIGN AND METHODS. Data are shown as a ratio of the control primers.

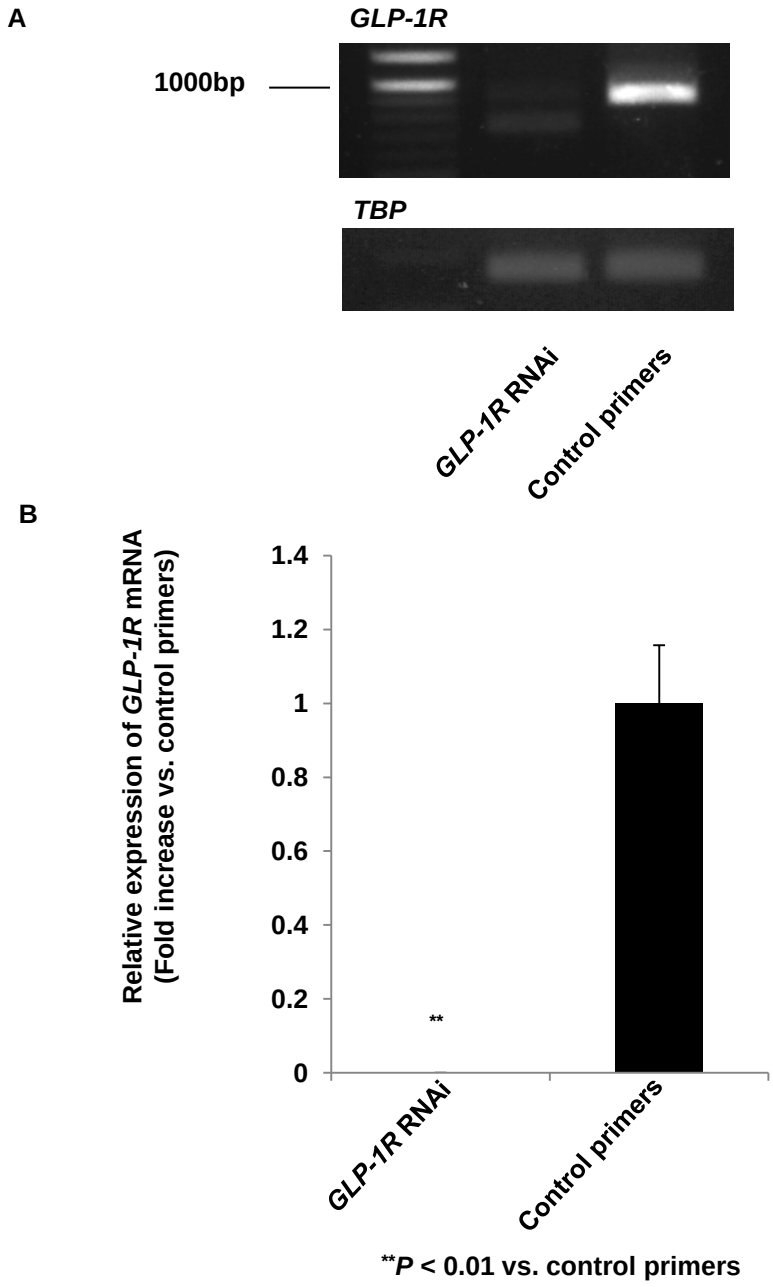

Supplemental Fig. 3

Induction of intracellular cAMP concentration by Ex-4 was examined in prostate cancer cells as described in RESEARCH DESIGN AND METHODS. After 24 h of serum deprivation cells were treated with 10 nM Ex-4 for 60 min. $^{*}P < 0.05$ vs. 0 min, $^{\#\#}P < 0.01$ vs. 0 min of the other cells.

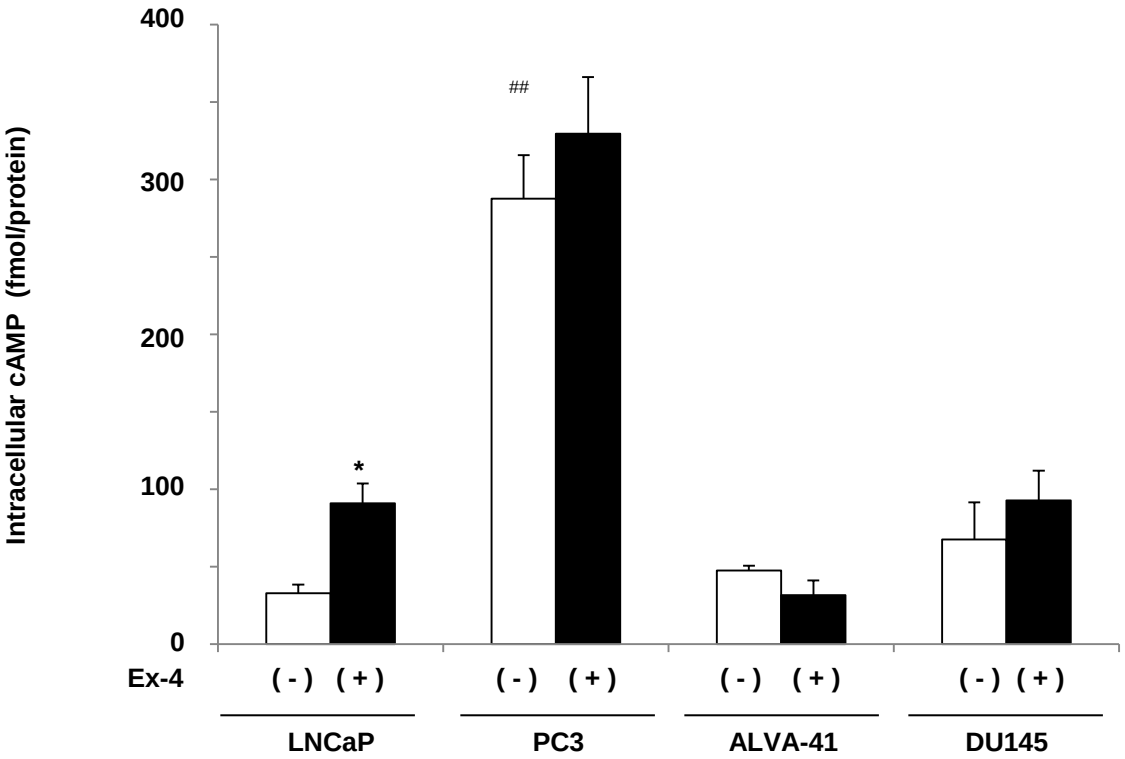

Cell proliferation assay was performed with LNCaP cells treated with (A) forskolin (0, 1 or 10 μM) and (B) PD98059 as described in RESEARCH DESIGN AND METHODS.
** $P < 0.01$ vs. control

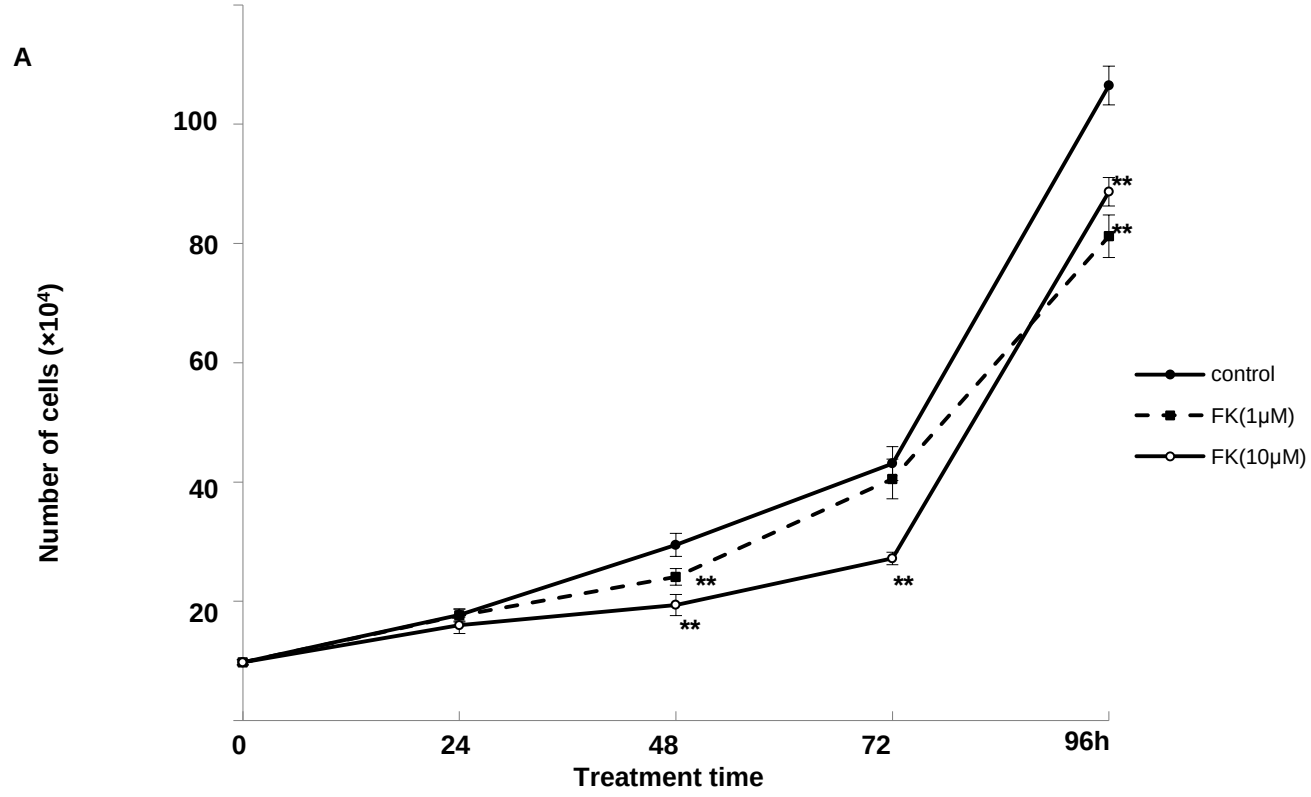

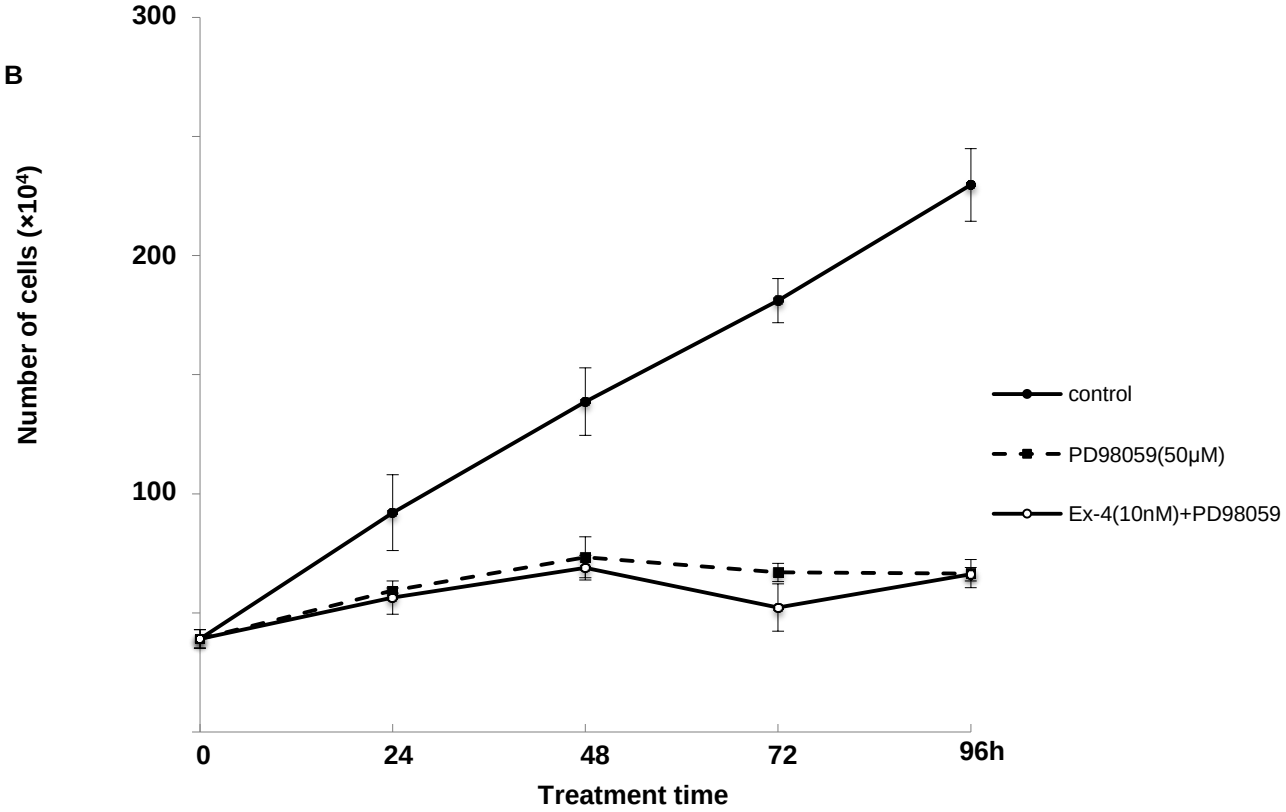

Supplemental Fig. 5

Reduction in phosphorylation of ERK-MAPK was examined in prostate cancer cells. (A) Cells maintained in media with 10% FBS were stimulated with 10 nM Ex-4 or saline for 15 min. (B) LNCaP cells maintained in media with 10% FBS were stimulated with 10 μM forskolin or DMSO for 15 min. Cell lysates were harvested and subjected to western blotting to assess phosphorylated ERK-MAPK and ERK-MAPK expression. Phospho-ERK-MAPK/ERK-MAPK protein levels were quantified by densitometry. Data were calculated from triplicate independent experiments and are shown as a ratio of LNCaP(-). Experiments were repeated at least three times. Unpaired *t*-tests were performed to calculate statistical significance ($^{*}P < 0.05$ vs. control).

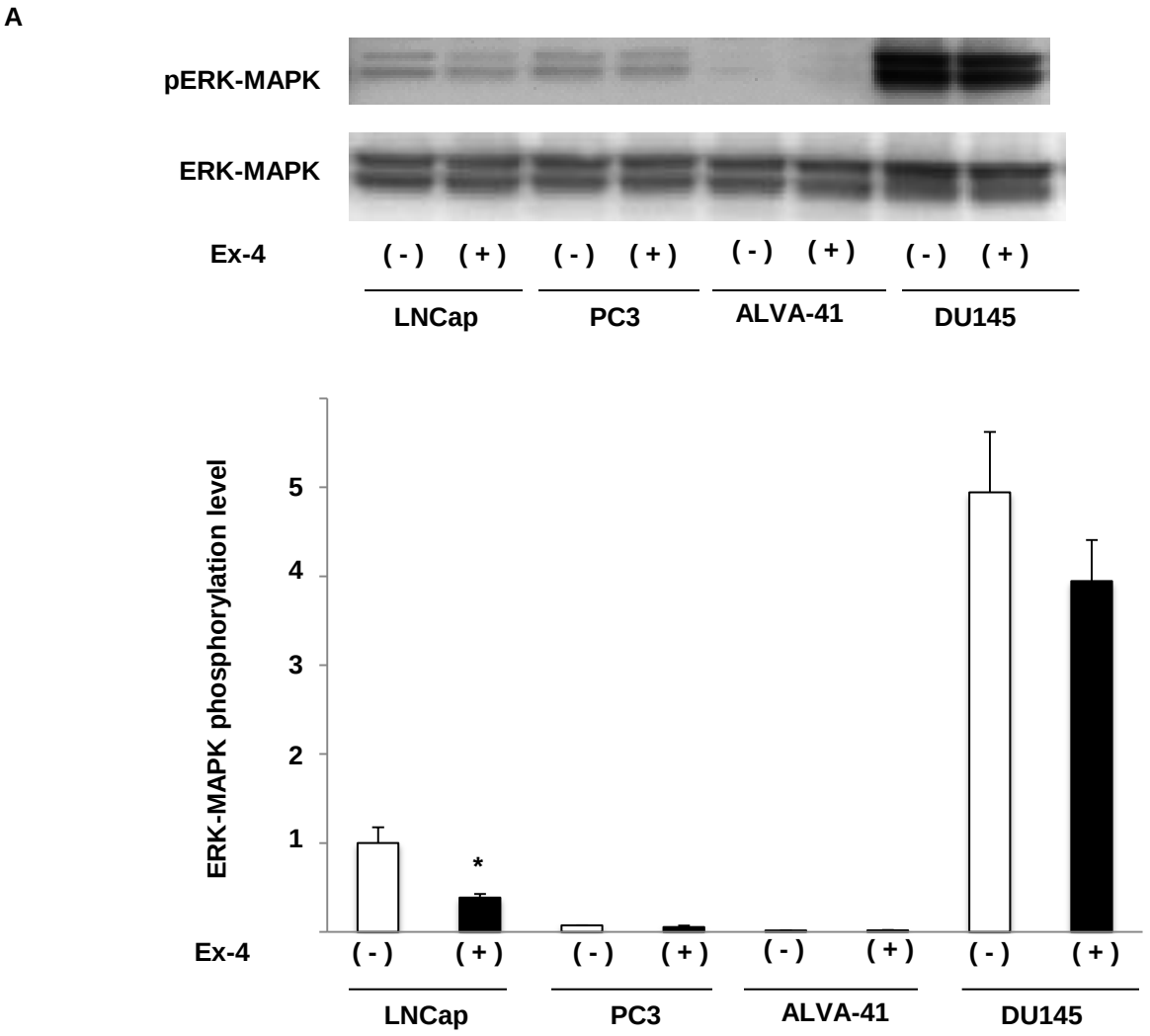

B

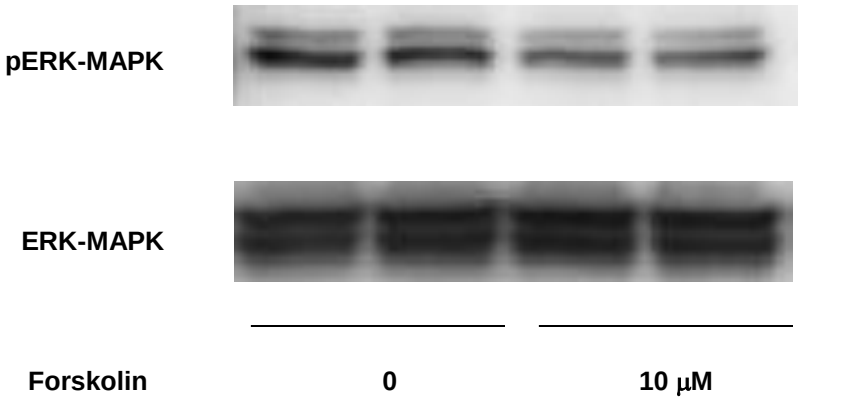
pERK-MAPK
ERK-MAPK
Forskolin
0
10 μM

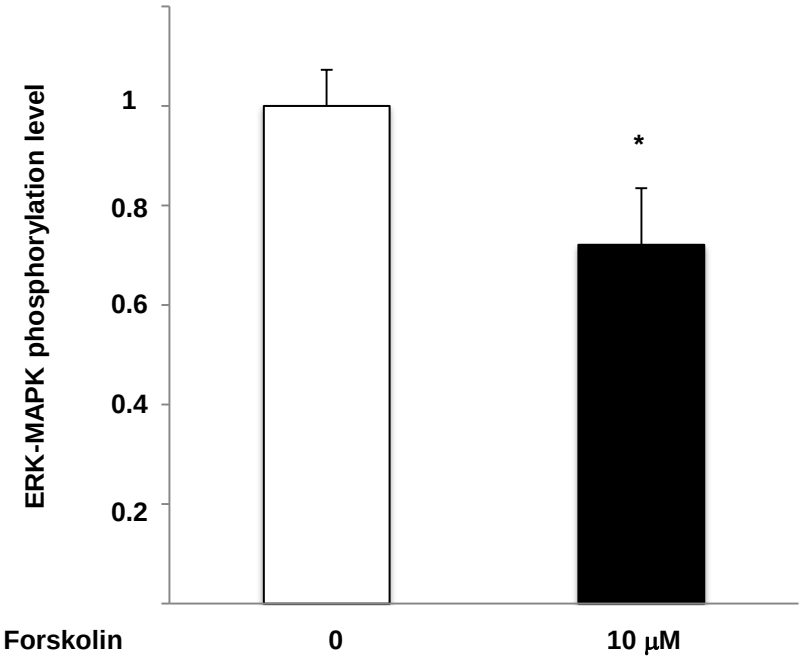
ERK-MAPK phosphorylation level
1
0.8
0.6
0.4
0.2
*
Forskolin
0
10 μM

Supplemental Fig. 6

LNCaP cells maintained in media with 10% FBS were treated with Ex-4 (0.1–10 nM) or saline for 15 min in the case of Akt activation detection, or 24 h for the examination of Caspase 3, Bcl-2, and BAD protein expression levels by western blotting. The following antibodies were used: phospho-Akt (Cell Signaling #4051) and Akt (Cell Signaling, #9272), Capspase 3 (Cell Signaling, #9662), Bcl-2 (Santa Cruz, sc-7382), BAD (Cell Signaling, #9292) and GAPDH (Santa Cruz, sc-20357). Caspase 3 control cell extracts (Cell Signaling, #9663) were used as a positive control for Caspase 3. Experiments were repeated at least three times.